A MODEL STUDY OF FLOW VELOCITIES
IN AN OXIDATION DITCH

By

UBBO AGENA

Bachelor of Science

Iowa State University

Ames, Iowa

1966

Submitted to the faculty of the Graduate College
of the Oklahoma State University
in partial fulfillment of the requirements
for the degree of
MASTER OF SCIENCE
May, 1968

A MODEL STUDY OF FLOW VELOCITIES

IN AN OXIDATION DITCH

THESIS APPROVED:

S. T. Nixon
Thesis Adviser

James E. Garton

N Durham
Dean of the Graduate College

PREFACE

The experimental investigations of this study were conducted with the financial support of the Oklahoma Agricultural Experiment Station Project 1208 and the research facilities of the Department of Agricultural Engineering.

My gratitude goes to the National Science Foundation through whose financial aid my program of study was possible.

Indebtedness is acknowledged to Dr. G. L. Nelson for his guidance and encouragement throughout this study.

Appreciation is expressed to the personnel of the research laboratory for their work in construction of equipment used in the experimental work. The assistance of the Agricultural Engineering Department draftsmen in the preparation of the illustrative materials contained in this thesis is also acknowledged.

TABLE OF CONTENTS

LIST OF TABLES

LIST OF FIGURES

Figure		Page

CHAPTER I

INTRODUCTION

The trend toward confined housing of farm livestock has associated with it the problem of management of animal wastes. Many waste disposal methods formerly used have become uneconomical or too time consuming for use today (19).

The oxidation ditch (or Pasveer oxidation ditch) has been advocated as a possible solution to the problem of animal waste disposal. The oxidation ditch is basically an extended-aeration activated-sludge process utilizing a rotor aerator to mechanically aerate a diluted waste slurry. The oxidation ditch offers advantages in economy of treatment and simplicity of operation over other aeration treatment alternatives.

Development of the oxidation ditch is credited primarily to Dr. A. Pasveer, who developed it for treatment of wastes from small municipalities in the Netherlands. Application of principles governing oxidation ditch operation for municipal sewage treatment to treatment of animal wastes cannot be made directly, due to the basic difference that exists in the wastes being treated, i.e.: "sewage is water which contains some solid matter, while manure is solid matter which contains some water" (26, p. 1).

CHAPTER II

LITERATURE REVIEW

Oxidation Ditch Components

The oxidation ditch consists of two basic components:

1. A ditch or channel in an oval or race track configuration
2. A rotor aerator

As developed for municipal sewage treatment, the oxidation ditch consists of a channel or number of channels for storage and circulation of wastes, commonly in an oval or race track layout. The channel is of rectangular or trapezoidal cross-section with a minimum bottom width of two feet and a liquid depth of about forty inches (18). Lining of the channel may be required to prevent seepage or for slope stability, depending on the soil conditions in which the ditch is built. Corners must be well rounded to prevent eddying and dead areas, and the outside edges of curves must be protected from erosion (16).

Construction of the aeration basin as a ditch rather than a tank has several advantages. Construction costs are held to a minimum, as the shallow ditch is easily constructed and the expense associated with construction of a large reinforced concrete tank is eliminated. For treatment of a given quantity of wastes, the land area required for the ditch is only slightly greater than for a conventional treatment plant, and is less than 10 percent of that required for lagoons. The water surface area exposed to aeration is not restricted to a small tank surface, resulting in a more complete utilization of the aeration capabilities of the rotor (2). Also, a quantity of oxygen supplementing that supplied by rotor operation may be absorbed directly from the air. The additional oxygenation supplied by surface absorption depends on the water surface area exposed to the atmosphere, and may be as high as 40 percent (16).

A modification of this design is commonly used in adapting the oxidation ditch to treatment of animal wastes. The ditch is constructed as a two-channel arrangement located under the slatted floor areas of a livestock building, as shown in Figure 1. The channels are constructed of brick or concrete, and are of rectangular cross-section. Location of the ditch under the slats eliminates some handling of wastes, since collection and transfer to the ditch becomes automatic (17).

Rotor aerators in common use are of from 26 to 36 inches in diameter, although one rotor being produced exclusively for agricultural applications is 16 inches in diameter (17). The rotor usually consists of approximately 12 blades radiating from and rotating about a horizontal axis. The blades are of a staggered tooth design, with the teeth on successive blades occupying the voids in the preceding blade (2). Blade design varies between rotors, with the oxygen transfer and liquid propulsion capabilities of a rotor depending greatly on the blade design. Common rotation speeds are from 60 to 120 rpm (revolutions per minute), although speeds of up to 200 rpm are being used (3, 17). The length of rotor required for a disposal system depends on the channel width, the required oxygenation rate, and the required liquid velocity.

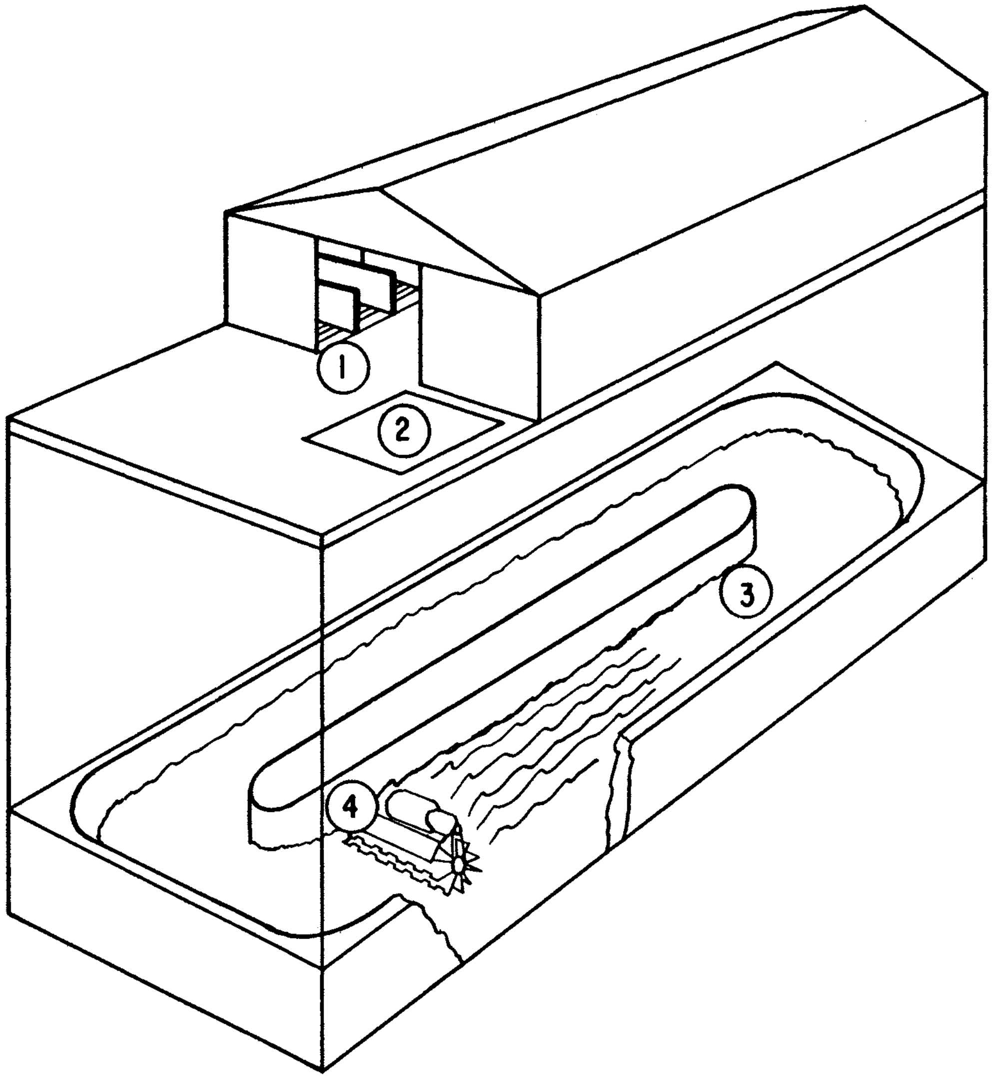

1. Manure falls through slatted floor into ditch
2. Aeration rotor is located outside of building to permit vapors to escape
3. Wastes circulate continuously in ditch
4. Aeration rotor aerates and circulates ditch contents

Figure 1. Design of Oxidation Ditch as Integral Part of Livestock Building (17)

Rotor operation is described by Berk (3, p. 3) as:

> As each blade passes through the water it exerts movement on the liquid. When the blade first strikes the liquid it exerts a downward force and with further rotation this is a horizontal force. As the blade leaves the water it lifts large quantities of the liquid out of the water for the induction of oxygen.

Thus, the rotor aerator functions to induce oxygen into the liquid and to propel and agitate the liquid.

Activated-Sludge Waste Decomposition

Decomposition of organic matter in a waste is accomplished primarily by micro-organisms which utilize the matter as food. Organisms involved include: bacteria, fungi, acitomycete, protozoa, algae, and phage (4).

In the oxidation ditch the primary decomposition of wastes is aerobic, meaning that the organisms utilize free oxygen in the liquid to accomplish this decomposition. The decomposition process is classified as an extended-aeration activated-sludge process (29).

The activated-sludge process of sewage treatment involves the aeration (by compressed air or mechanically) of a mixture of a screened, presettled, or otherwise primary-treated sewage mixed with a small volume of previously aerated sludge, called activated sludge. The activated sludge supplies aerobic bacteria (and other organisms) to the sewage and adsorbs suspended and colloidal matter from the mixture. After aeration of the sewage and sludge mixture (called a mixed liquor), the mixed liquor is transferred to a settling tank where sludge settlement occurs. After settlement, the clear effluent is discharged from the settling tank and a portion of sludge is returned to the aeration tank, with the remaining sludge being wasted (13).

Aeration of the mixed liquor is usually from 4 to 8 hours in length, with 6 hours being most common. Two processes occur during the aeration period. First, adsorption of solids by the sludge and clarification of the mixed liquor takes place. Then, biological oxidation of the adsorbed organic matter occurs (25).

For animal waste treatment, the period of time for aeration in an oxidation ditch is greater than for the conventional activated-sludge process. The extended-aeration process is used since wastes entering the ditch commonly undergo no primary treatment and since sludge is removed from the ditch only on a periodic basis (25).

Oxidation of wastes in the extended-aeration activated-sludge process occurs in two steps:

1. A partial oxidation of adsorbed organic wastes
2. Oxidation of dead biological cells in the sludge

The total oxygen demand associated with the extended-aeration process is greater than that of the conventional aeration process, since the extended-aeration process requires oxygen for decomposition of dead biological cells, in addition to the oxygen required for decomposition of the waste matter (29).

Animal Waste Characteristics

Physical, chemical, and biological properties of an animal waste must be considered in determining the suitability of using an oxidation ditch for treatment of the waste.

Physical properties are those properties a waste possesses which are related to the physical composition of the waste, such as density and viscosity. These properties determine the flow behavior of the waste and affect its sedimentation and flocculation rates.

The chemical properties of a waste are determined by its chemical composition. Chemical properties determine the potential value a waste has as fertilizer and often determine whether a treated effluent will cause pollution (18).

Biological properties deal with both the biological constituents composing the waste and the properties the waste possesses which affect its ability to be decomposed by bacteria. Biological properties are commonly used as the basis for calculation of oxygen requirements for aerobic treatment of the waste, although chemical properties may be used (26).

Although much research has been devoted to determining the properties of animal wastes, large differences exist in values obtained for the properties. These differences exist because the properties of a waste are affected by animal physiology, rations being fed, animal environment, and conditions and methods involved in collection and evaluation of samples (26).

In considering effects animal waste properties will have on oxidation ditch operation, it must be remembered that the major portion of the effluent in an oxidation ditch consists of partially decomposed wastes and dilution water added from other sources. Thus, the effluent in the ditch will exhibit properties considerably different from those of fresh animal manure.

Physical Properties

Much early research into animal waste properties dealt with the waste's physical properties, as these properties were felt most important. Results of this early research do not adequately represent present conditions, as improved feed rations and decreased use of bedding have decreased the volume and changed the composition of animal wastes (26).

In recent research on physical properties of fresh and diluted dairy and poultry wastes, Sobel (24) categorized physical properties into the following general areas:

1. Basic physical composition-moisture content, volatile solids, and fixed (involatile) solids
2. Particle density and bulk density
3. Production per animal per day
4. Particle size and distribution
5. Dilution and its effect on flow properties
6. Settling rate and effect of dilution on settling rate
7. Suspended and dissolved solids
8. Flowability
9. Freezing point

Many papers dealing with animal wastes give values to some of these properties, particularly production per animal, basic physical composition, and suspended and dissolved solids (6, 8, 10, 26). Other studies have evaluated the properties indirectly by research on methods of handling the waste, such as pumping of manure slurries (10, 11, 27).

Chemical and Biological Properties

Much information on chemical properties of animal wastes is available, with most early studies having been conducted on the fertilizing value of animal wastes. As a result, much information has been gathered on the nitrogen, potassium, and phosphorus contents of an animal waste (7, 19, 26). In recent years the concept of disposal of wastes by biological and chemical treatment has focused attention on the chemical oxygen demands of the waste (26), as well as the effects chemical substances (such as nitrates) present in minute amounts may have on the method of treatment used (18, 28).

The COD (chemical oxygen demand) of an effluent is a measure of the amount of oxygen required to chemically oxidize the total organic compounds in the effluent. Although exact testing procedures for determining the COD of a waste vary, the general procedure followed is to boil a sample of waste with a strong oxidizing agent (such as potassium dichromate) under acid conditions and determine the amount of oxygen used in the reaction (26). COD values depend mainly upon the chemical composition of the effluent, and may often best represent the total oxygen demands of the waste. Values of COD are commonly given along with BOD (biological oxygen demand) values.

Knowledge of biological properties of animal wastes is essential in considering the use of a disposal system utilizing biological decomposition for reduction (whether partially or completely) of the volume of decomposable organic matter. The biological property of BOD is commonly used to determine the suitability of using a method of biological treatment of the waste, although COD or PE (population equivalents) may be used (26).

The BOD of a waste is defined by Curtis (5) as: "the amount of oxygen required by bacteria while stabilizing decomposable organic matter under aerobic conditions." Thus, a BOD determination gives a measure of the biologically oxidizable organic matter found in the waste.

Although many different procedures are common in performing the BOD test on a waste, the underlying principle is the same (28). A sample of waste is mixed at various dilutions with fully aerated tap (or distilled) water, inoculated with bacteria if necessary, and incubated at a constant temperature for a given period of time (commonly 20° Centigrade and 5 days). The dissolved oxygen concentration is measured at the beginning and end of this period, and the BOD commonly expressed as the weight of oxygen used per volume of waste (such as milligrams of oxygen per liter of waste).

The BOD values obtained depend on several factors, including:

1. Bacterial composition of the effluent
2. Presence of bacteriostatic agents (bacterial growth inhibitors) in the waste
3. Presence of substances subject to direct oxidation (such as nitrites) in the effluent

Values of BOD and COD for animal wastes have been determined by various researchers (18, 26, 30).

The BOD to COD ratio reflects the percentage of organic matter present in a waste which is biologically decomposable (26). This ratio is commonly used in analysis of partially decomposed wastes.

The PE (population equivalent) of an animal waste is defined as the number of humans required to produce wastes with a strength equivalent to that produced by an animal over the same period of time. The strength measurement is commonly on the basis of BOD values, although it may also be on the basis of dry matter content or carbon to nitrogen ratio of the wastes (26).

Oxidation Ditch Operation

Operation of the oxidation ditch depends upon the purpose for which the ditch is designed. As given by Morris (18, p. 29), "the oxidation ditch can be used to treat, partially or 'completely' or to store livestock manures aerobically."

The volume of wastes an oxidation ditch is capable of treating is dependent mainly on the biological oxygen demand of the wastes. From studies of operating oxidation ditches, Morris (18) concluded that for grain fed livestock (hogs and poultry), the BOD_5 (BOD as determined in a 5-day test at 20°C) adequately describes the total BOD of the waste. For roughage fed livestock (cattle and dairy cows), Morris feels the BOD_5 does not describe the total BOD of the waste and the COD (as usually determined) may not even adequately describe the total BOD if lignified material is present. Failure of COD to adequately describe total BOD may occur as lignified material is an insoluble nutrient having a very high oxygen demand when decomposed under aerobic conditions (28).

Morris (18) indicates an oxygen content of 1.33 times the total BOD of the wastes will be adequate for "treatment" of the wastes. However, Scheltinga (23) states that for complete treatment of wastes in a standard ditch operated by unskilled personnel, a ratio of oxygen content to total BOD of less than 2 is risky. The oxygen required per pound of waste BOD would be less than the above values for a ditch being used for aerobic storage of wastes.

Two systems of operation are common in treatment of animal wastes in an oxidation ditch (17). They are:

1. Batch (or intermittent)
2. Continuous

Under the "batch" system of operation the rotor is periodically stopped and the ditch partially emptied, commonly by a vacuum tank wagon. This system allows a manure volume of up to 4 percent of the total ditch volume to be added daily.

The "continuous" system requires that an amount of liquid be drained off daily equal to from 1 to 4 times the daily volume of animal wastes added to the ditch, the exact volume drained off depending on both the volume of wastes added and the volume of water added from other sources. Morris (17) recommends that the daily addition of manure not exceed 1.5 percent of the total ditch volume.

The ditch volume required per animal-day (based on the above recommendations) is:

	System of Operation	
Animal Unit	Batch	Continuous
100 lb swine	7 cu ft	10 cu ft
1000 lb cattle	50 cu ft	70 cu ft
5 lb poultry	1 cu ft	1.5 cu ft

The accuracy of these estimated volume requirements appears open to question, as Irgens and Day (12) recommend a ditch volume of 6 cu ft for wastes from a 125-lb pig for ditch operation under the continuous system.

At present, it is not known whether complete treatment of animal wastes in an oxidation ditch will be economical. While Linn (17) indicates that complete treatment is feasible, Hart (9) reports it is uneconomic to expect endogenous and complete stabilization of wastes.

Operation of the ditch as an aerobic waste storage tank may prove profitable, even if complete stabilization and degradation does not occur. Storage of wastes aerobically offers the advantages of being odor-free and unattractive to flies (12).

Inclusion of a sedimentation pit in an oxidation ditch utilized for aerobic waste storage should increase its storage capacity. Some solid waste particles could be collected in and removed from the sedimentation pit, thereby reducing the organic matter of the waste effluent and consequently reducing the oxygen requirement for treatment of waste effluent circulating in the ditch (30).

Liquid Velocity

Velocity Requirements

The velocity of liquid flow in an oxidation ditch must be great enough to prevent sedimentation of waste particles along the ditch length. Thus, the velocity must be sufficient to either keep all solid particles in suspension or to transport them along the ditch bottom to a sedimentation pit for eventual removal.

Research on velocity requirements for agricultural wastes is lacking. Present recommendations (18) are based on experience with oxidation ditch treatment of municipal sewage and call for a minimum surface velocity of 1 foot per second.

The accuracy of these recommendations is questionable. Babbitt and Baumann (1) state that a velocity greater than 0.5 feet per second is generally sufficient to keep most organic matter in suspension. In velocity studies of an oxidation ditch containing swine wastes, Knight (13) observed that waste particles lying on the channel bottom were picked up and carried in suspension at all rotor speeds and immersions tested. In research on ditches containing municipal wastes, Pasveer (21) found some sludge deposition occurred with liquid velocities of less than 25 cm per second in the middle of the ditch. However, although anaerobic conditions existed in this sludge, no interference with the overall purification process was noted.

Previous Velocity Studies

A literature review indicates little research has been conducted on the relationship between liquid velocity in an oxidation ditch and the design and operating conditions of the ditch and rotor aerator. A study by Knight (13) on an oxidation ditch at the Iowa State University Swine Nutrition Farm at Ames, Iowa was the only thorough ditch velocity study found.

The ditch used in Knight's work had a flat bottom with sloping sides, and was approximately 4 feet deep at the center and 14 feet wide at the top. It was built in an oval arrangement and lined with a combination of cationic asphalt and polyethylene sheeting. A plan of the ditch is shown in Figure 2.

The rotor used was a 27 1/2-inch diameter cage rotor 3 feet long. The rotor and variable speed drive unit were constructed and supplied by Lakeside Engineering Company, Chicago, Illinois. The rotor was

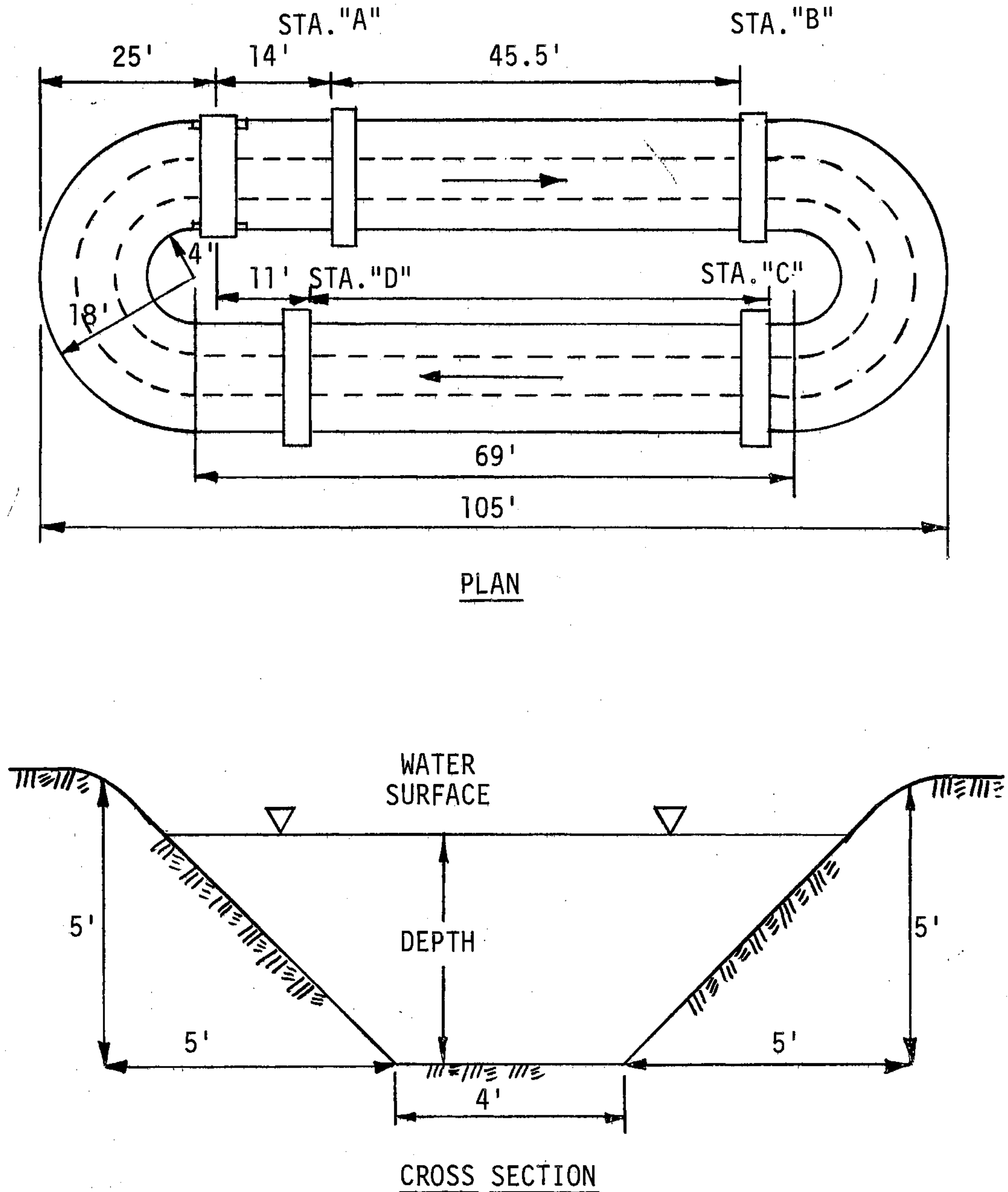

Figure 2. Oxidation Ditch at Iowa State University Swine Nutrition Farm (13)

positioned across a straight section of ditch as shown in the ditch plan in Figure 2. Screw jacks were used for mounting the rotor on the rotor platform, enabling rotor position to be adjusted vertically while keeping its plan location stationary. Details of the rotor construction are given in Figure 3.

Velocity measurements were taken (using current meters) at the four stations A, B, C, and D shown in the plan mentioned previously, Figure 2. At each station measurements were taken at the ditch center-line and at locations 2 and 4 feet on each side of the center-line. At each location measurements were taken just below the water surface, 5 inches above the ditch bottom, and at one or two levels between the surface and bottom readings. The measurements at these depths at a particular location constitute one velocity profile.

Velocity profiles were determined at each station for rotor immersion depths of 3, 6, 9, and 12 inches and rotor rotation speeds of 60 and 100 rpm. Typical velocity profiles obtained are shown in Figures 4 and 5. The average velocity at each vertical profile line was determined by measuring the area between each velocity curve and the zero datum and dividing this area by the depth at that station. The average velocities obtained are given in Table I.

High surface velocities and low bottom velocities were found at station A, which was located near the rotor. Knight's results indicated the velocity at any depth at station A may differ considerably from the average velocity, while at station D the average velocity gave a good indication of the velocity at any depth in the profile.

The average velocity was greater for the higher rotor speed at the 3-, 6-, and 9-inch immersions, with the difference in velocities at the

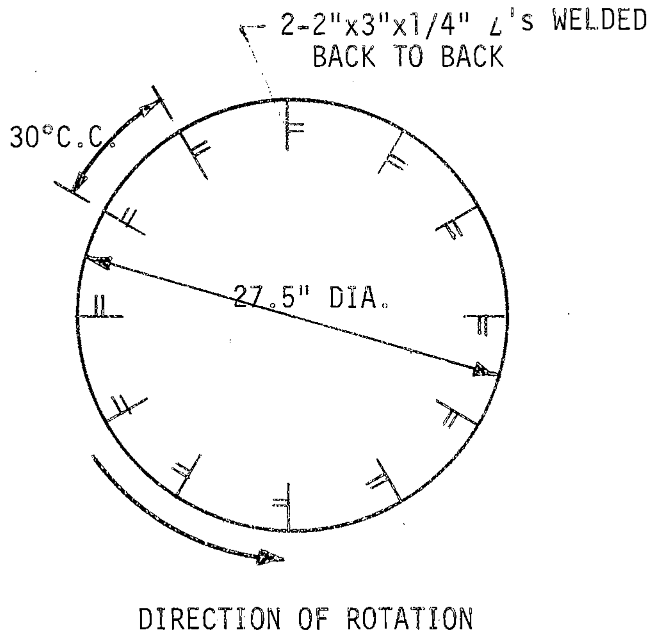

END VIEW

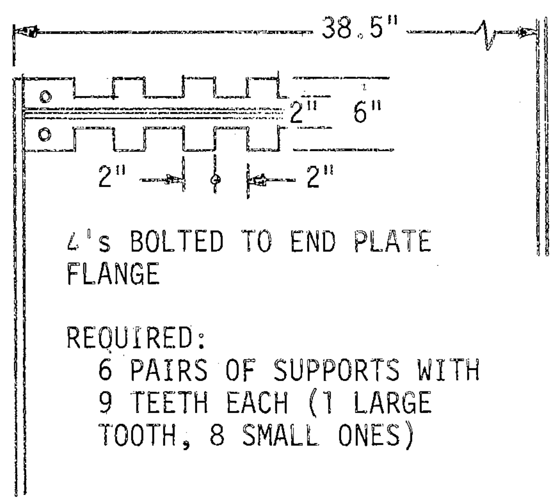

SIDE VIEW

Figure 3. Details of Cage Rotor Studied by Knight (13)

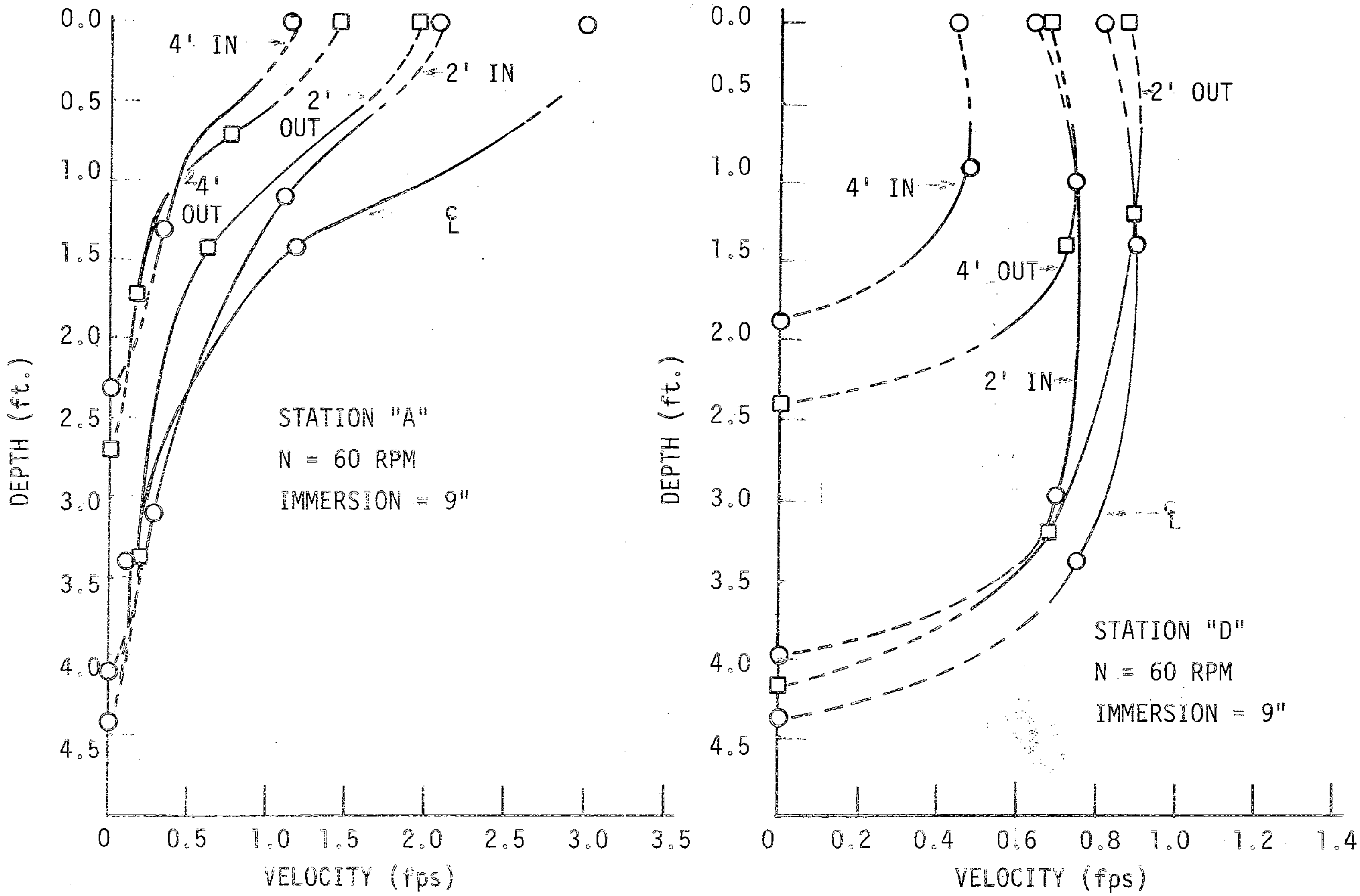

Figure 4. Typical Velocity Profiles Found by Knight (13)

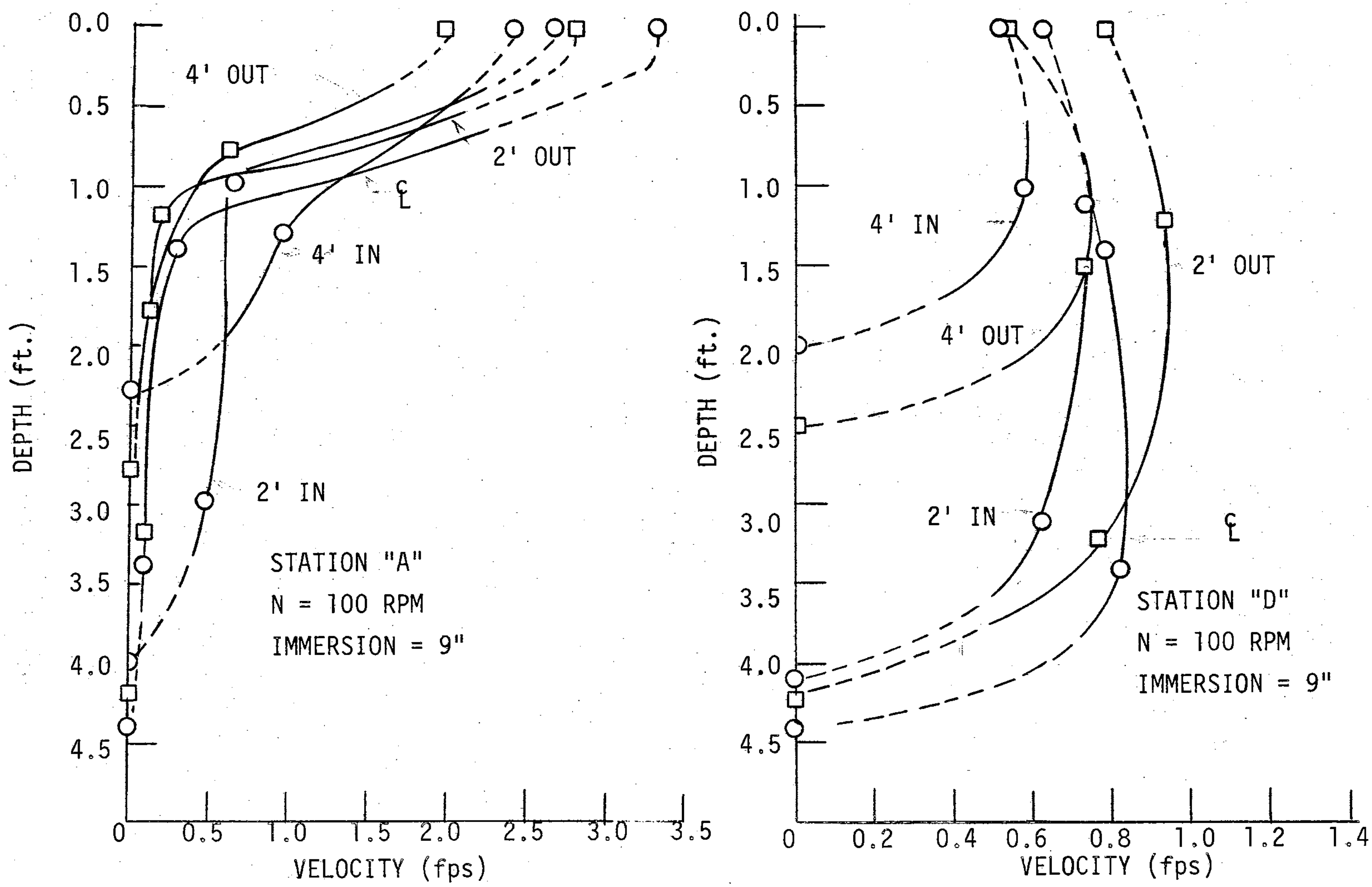

Figure 5. Typical Velocity Profiles Found By Knight (13)

TABLE I

RESULTS OF MEAN VELOCITY STUDIES (13)

Rotor Speed (rpm)	Profile Station	Immersion Depth (in)	Avg. Velocity At A Vertical Line 4' in (fps)	2' in (fps)	℄ (fps)	2' out (fps)	4' out (fps)
60	A	3	0.27	0.45	0.86	0.37	0.44
		6	0.55	0.52	1.04	0.57	0.82
		9	0.51	0.83	1.01	0.61	0.52
		12	0.54	0.57	0.92	0.55	0.52
	B	3	0.63	0.48	0.41	0.48	0.50
		6	0.84	0.61	0.52	0.65	0.65
		9	0.86	0.70	0.58	0.75	0.63
		12	0.76	0.60	0.54	0.56	0.62
	C	3	0.19	0.40	0.47	0.59	0.47
		6	0.43	0.54	0.64	0.73	0.76
		9	0.37	0.57	0.72	0.87	0.67
		12	0.36	0.61	0.62	0.67	0.70
	D	3	0.24	0.46	0.51	0.59	0.44
		6	0.45	0.62	0.75	0.89	0.68
		9	0.41	0.69	0.81	0.66	0.66
		12	0.47	0.56	0.69	0.70	0.63
100	A	3	0.72	0.62	0.91	0.56	0.60
		6	0.81	1.23	1.17	0.44	0.94
		9	1.23	0.78	0.67	0.49	0.58
		12	1.25	0.77	0.69	0.61	0.73
	B	3	0.88	0.62	0.50	0.66	0.74
		6	1.06	0.75	0.62	0.74	0.88
		9	0.99	0.68	0.52	0.55	0.61
		12	0.94	0.58	0.46	0.45	0.47
	C	3	0.38	0.56	0.63	0.83	0.63
		6	0.49	0.71	0.73	0.80	0.85
		9	0.52	0.58	0.55	0.78	0.82
		12	0.34	0.50	0.52	0.66	0.73
	D	3	0.30	0.63	0.76	0.75	0.59
		6	0.53	0.71	0.93	0.94	0.81
		9	0.51	0.64	0.76	0.81	0.64
		12	0.45	0.50	0.65	0.66	0.58

high and low speed being greatest at the 3-inch immersion. At the 12-inch immersion the average velocity was greater for the lower rotor speed.

The average velocity at each profile was highest at the 6- and 9-inch immersions, with the velocity at the 12-inch immersion greater than at the 3-inch but lower than that at the 6- and 9-inch immersions.

Velocities at station C were found to be much higher on the outside of the ditch center-line than on the inside. This was also true at station D, although the velocity difference was less.

Rotor Power Requirements

The total power requirement for operation of an aeration rotor is composed of several components, which are:

1. Power required to overcome losses in the motor and drive system
2. Power required to overcome losses in rotor bearing mounts
3. Power utilized in transfer of oxygen to the liquid
4. Power utilized in agitation and circulation of the liquid

Power requirements to overcome losses in the motor and drive system and in the rotor mounts is dependent on the mechanical system utilized in mounting and driving the rotor and can be classified as "power requirements due to mechanical design".

The power utilized in oxygen diffusion and in agitation and propulsion of the liquid depends on the rotor and channel operating conditions and is commonly called "net rotor power requirements". The net rotor power requirement is commonly determined by subtracting the power required for rotor operation in air from the power required for rotor operation in the liquid (17).

Net rotor power requirements have been measured in several studies conducted to determine the most efficient rotor design for diffusion of oxygen into the liquid. For an aeration rotor, oxygen diffusion efficiency is commonly stated in terms of pounds of oxygen diffused per killowatt of power used. These studies were conducted in rectangular tanks, thus not accurately measuring the power requirements for agitation and propulsion of liquid in an oxidation ditch (13, 15, 18).

Results of these studies indicated the portion of blade directly adjacent to the rotor axis consumed power without adding appreciably to the oxygen diffusion of the rotor. The cage rotor (manufactured by Lakeside Engineering Company, Chicago, Illinois) was designed using this information to increase its oxygen diffusion efficiency by eliminating the center blade sections (3). Figures 6 and 7 give results of research conducted for a rotor with rectangular teeth and for a cage rotor (18). The terms used in these results are: OC is oxygen content in grams O_2 per hour, N is rotor power requirement in killowatts, OC per m rotor is oxygen content per meter rotor length in grams O_2 per hour per meter, N per meter m is rotor power requirements in killowatts per meter rotor length, and OC/N is oxygen content per unit rotor power requirement in grams O_2 per killowatt-hour.

Knight's (13) research (mentioned previously under section on liquid velocity studies) measured net rotor power requirements for several paddle immersion depths and rotor speeds. Figures 8 and 9 give results of this study. As expected, rotor power requirements increase

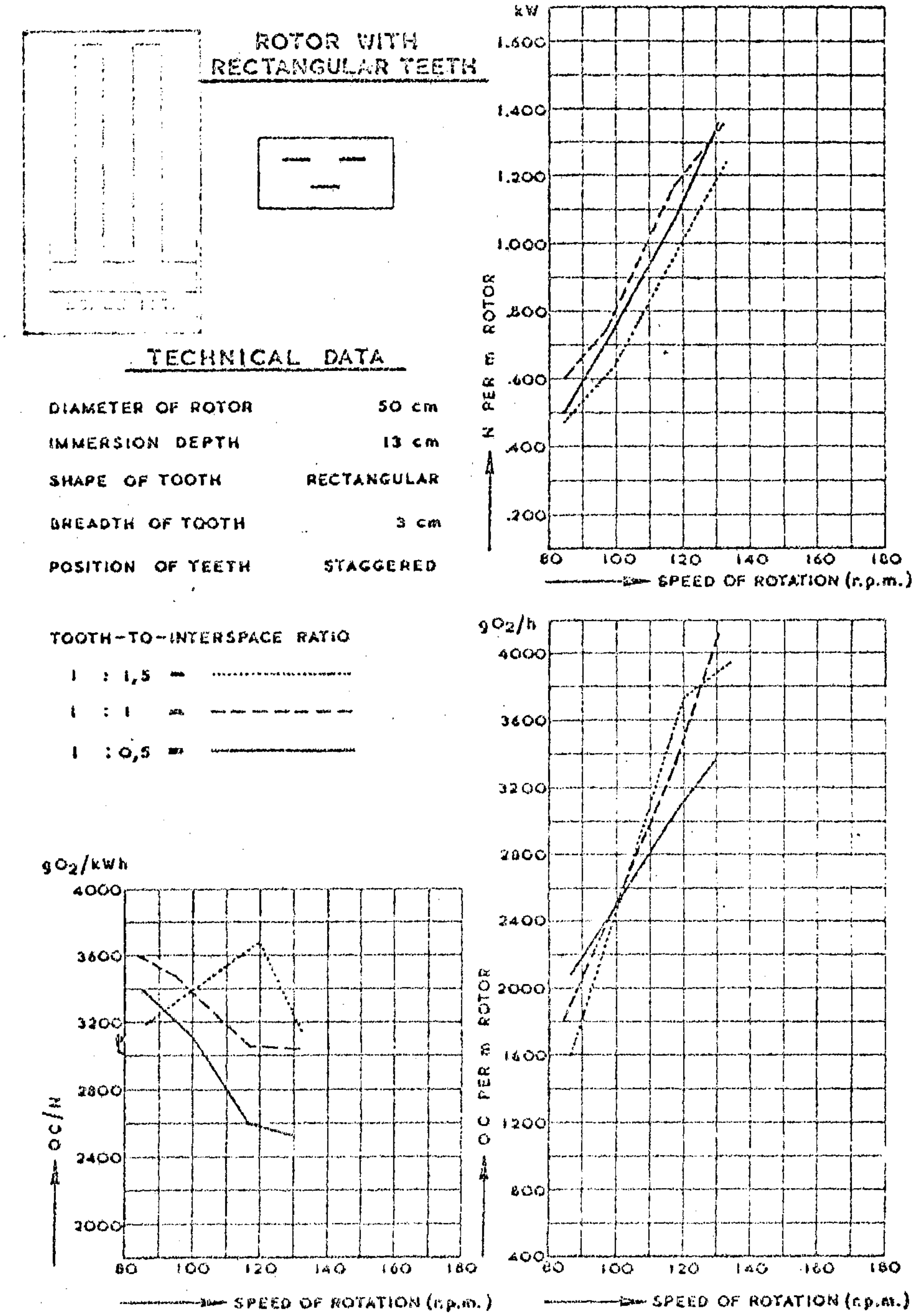

Figure 6. Results of Tests on a Rotor with Rectangular Teeth (18)

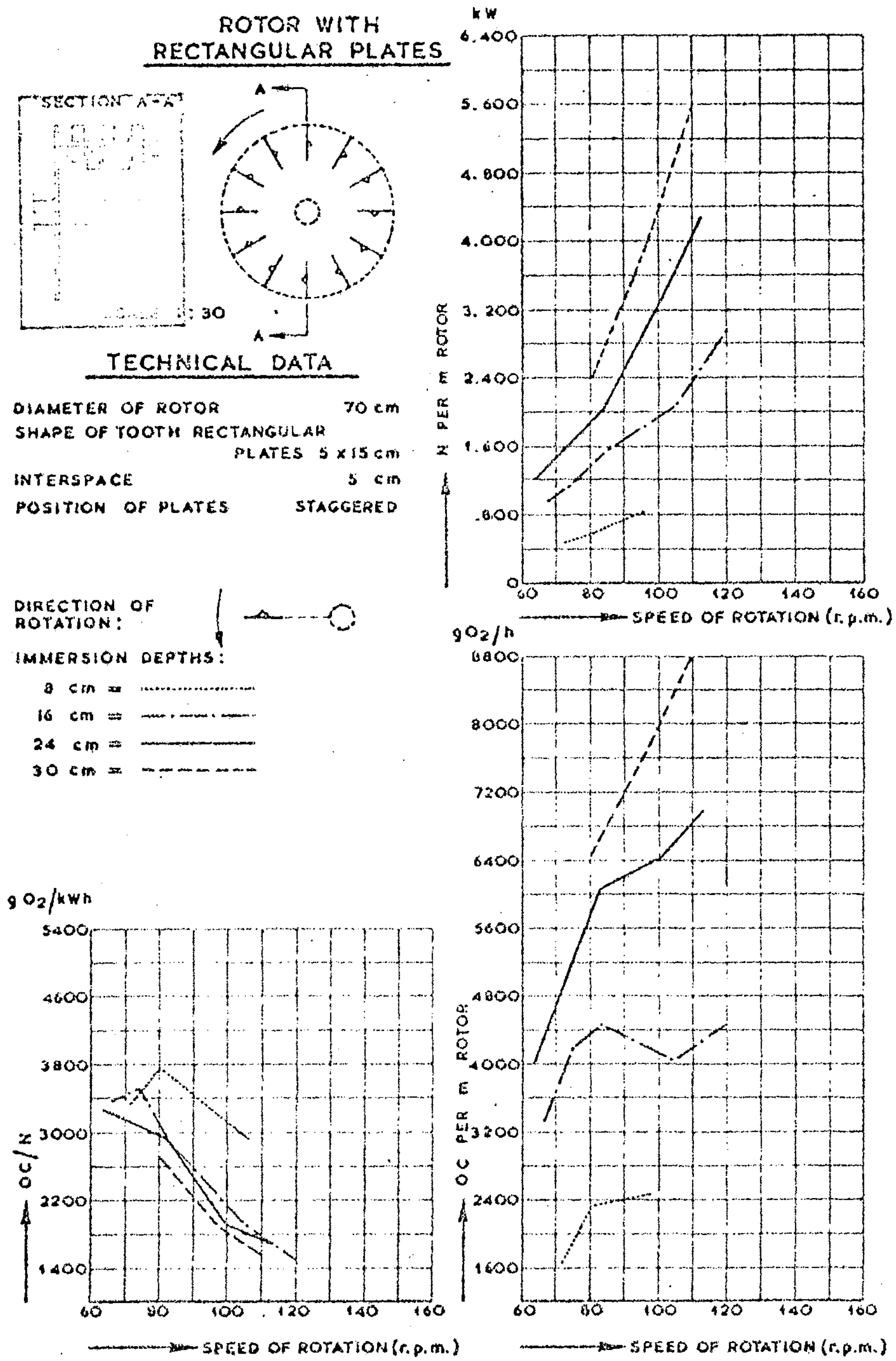

Figure 7. Results of Tests on a Cage Rotor (18)

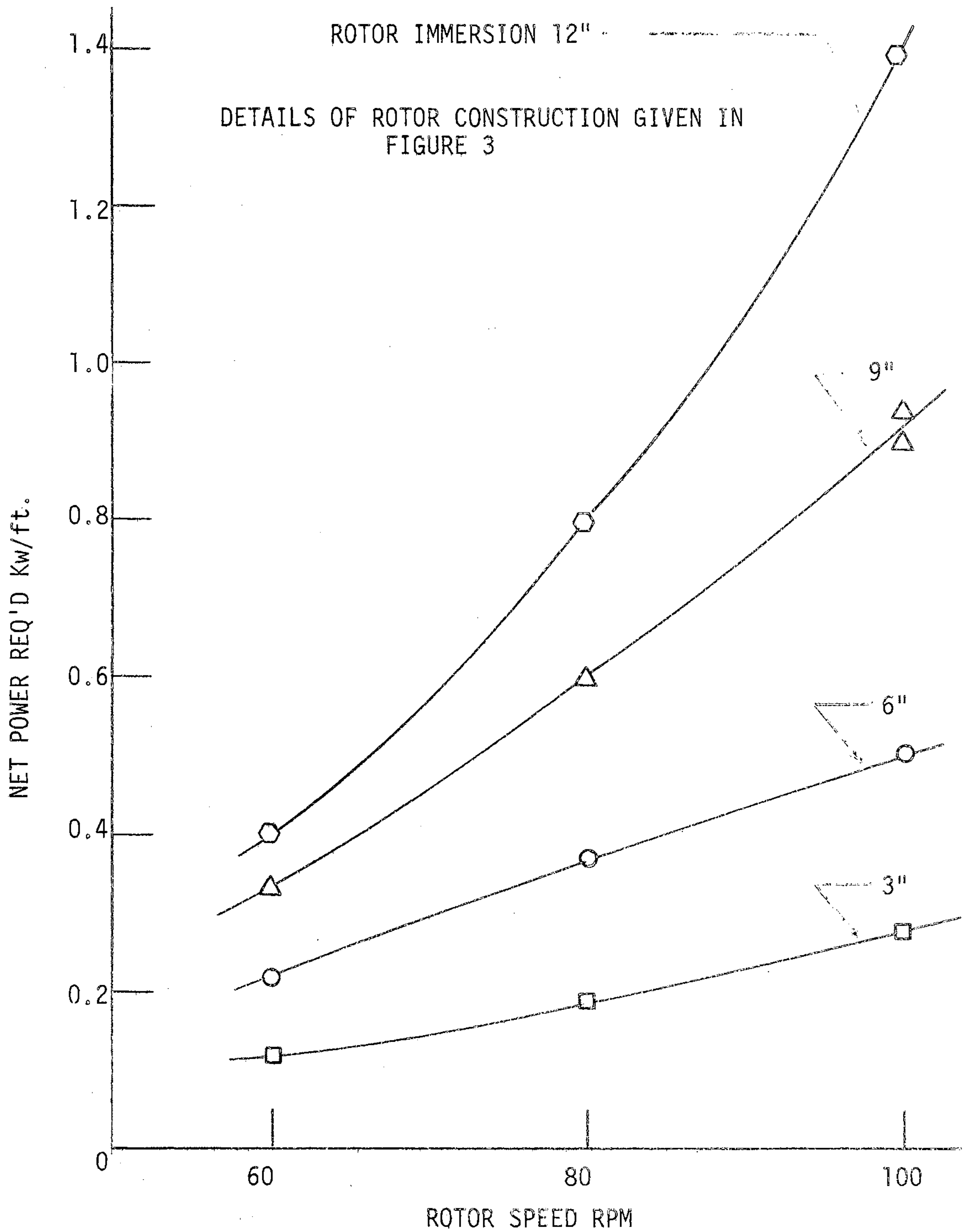

Figure 8. Results of Rotor Power Study By Knight (13)

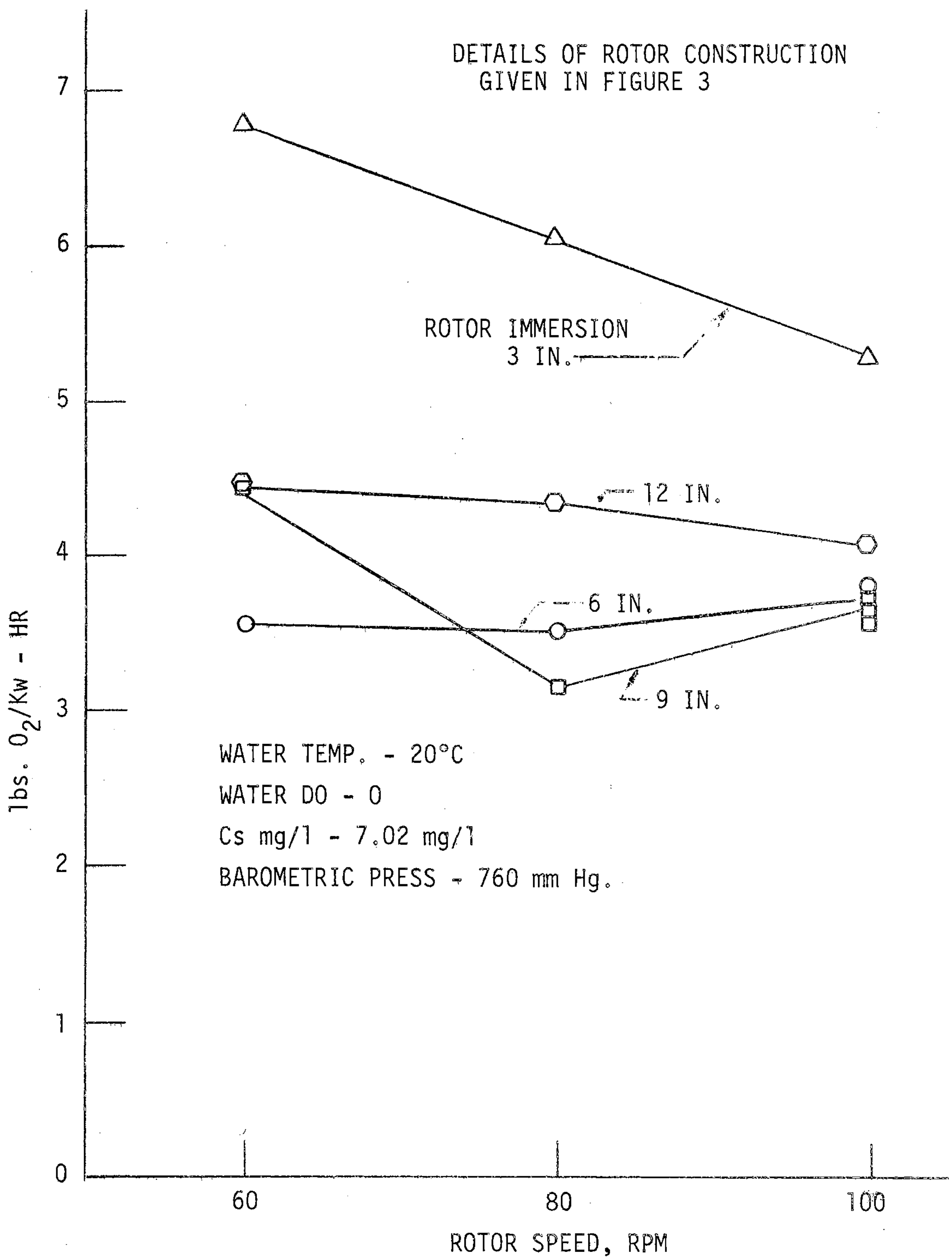

Figure 9. Results of Rotor Power Study by Knight (13)

as either rotor speed or paddle immersion depth is increased (16). In comparing his results with those of tests conducted on a similar rotor in a rectangular tank, Knight found most of the net rotor power values measured for the oxidation ditch to be lower than corresponding values found in the rectangular tank (13).

Rushton (22, 28) analyzed rotor power requirements for several impeller designs operating completely submerged in unaerated water. Turbine, propeller, and paddle impellers were included in the study, with impeller rotation being about a vertical axis in a vertical, cylindrical, flat-bottomed tank.

This study indicated that, for geometrically similar equipment an equation for impeller power could be developed utilizing dimensionless constants and a factor K (known as the Rushton factor). The developed equation is:

$$\frac{P}{\rho\, n^3\, D^5 Ne} = K \left(\frac{Ne\, \rho\, D^2\, n}{\mu}\right)^a \times \left(\frac{Ne\, D\, n^2}{G}\right)^b$$

where

P = net rotor power

K = Rushton factor - coefficient which is constant for a particular system

a & b = exponents which are constants for a particular system

ρ = liquid mass density

μ = liquid absolute viscosity

n = rotor speed

D = rotor diameter

G = gravitational effect

Ne = Newton's Second Law Coefficient

For this equation, an impeller Reynold's number $(\frac{Ne\ \rho\ D^2\ n}{\mu})$ of less than 10 indicates a truly viscous flow and a value of over 10,000 indicates a fully turbulent flow, with an intermediate zone for values between these limits.

In practice, existence of turbulent flow is generally assumed for points in the immediate vicinity of the impeller, with the state of flow found in other parts of the system depending on the characteristics of the system.

Rotor Aeration Studies

The rate at which oxygen is transferred to a waste material frequently controls the rate at which aerobic decomposition of its organic matter proceeds. Much research has been devoted to determining the physical processes involved in transfer of oxygen into a liquid and the factors affecting the rate at which this transfer occurs (3, 13, 21, 28). The following factors are generally considered of major importance:

1. Area of gas-liquid interface
2. Temperature
3. Time of contact
4. Intensity of agitation
5. Dissolved oxygen deficit

The oxygenation capacity of an aeration unit is commonly defined as the rate of oxygen transfer achieved by the unit when operating in distilled water under the conditions of 10°C, 760 mm atmospheric pressure, and zero dissolved oxygen content (21).

Several methods are available for determining the oxygenation capacity of an aeration unit at these conditions. A chemical such as sodium sulfite may be added in excess to deaerate the water and the oxygen transfer rate determined by measuring the rate of depletion of excess chemical as the aeration unit is operated. Mechanical methods of deaeration may be used to keep the water at zero dissolved oxygen while an aeration unit is tested. Also, the oxygenation capacity may be found by first determining the change occurring in the dissolved oxygen concentration of a volume of water while operating the aeration unit for a period of time. By use of suitable equations, this rate of concentration change can be converted into oxygenation capacity at standard conditions (13).

Aeration devices are commonly compared by use of operating efficiency comparisons. The operating efficiency of an aeration unit is defined as the pounds of oxygen (may be in grams) the unit will transfer per killowatt-hour of power used when operating in distilled water at 10°C (sometimes 20°C), 760 mm atmospheric pressure, and zero dissolved oxygen content. Use of operating efficiencies allows economic comparisons to be made between various aeration devices (13, 28).

The oxygenation capacities of various aeration rotor designs have been determined, with most work having been conducted in rectangular tanks. Results of this research have been summarized by Pasveer, Knight, and Morris (13, 18, 21).

Knight (13) conducted a study of the oxygenation capacity of a cage rotor in a prototype ditch. Results of this study are given in Figure 10, with the operating efficiency of this rotor given previously in Figure 9 (under net rotor power requirement study).

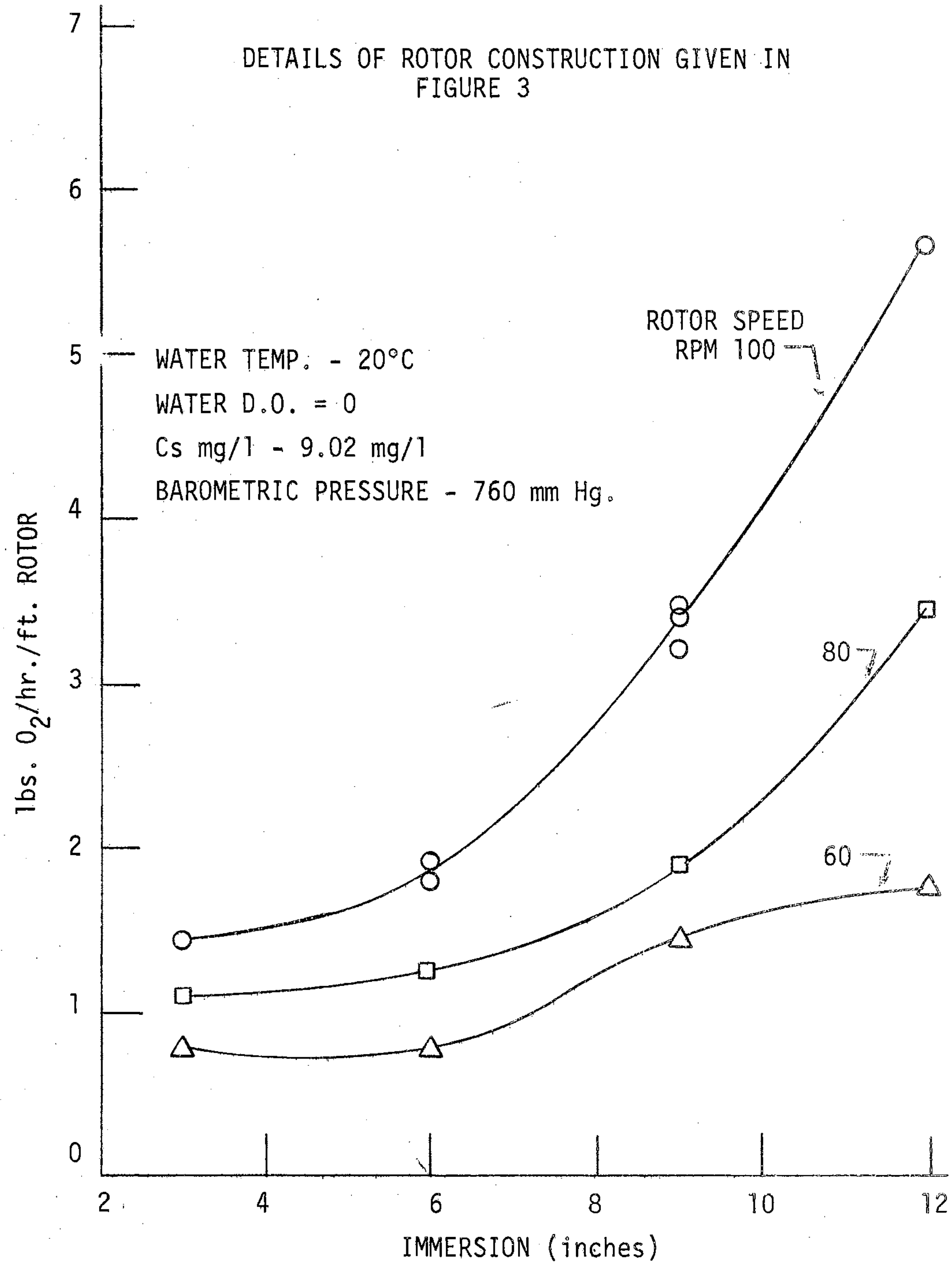

Figure 10. Result of Oxygenation Capacity Study of Cage Rotor (13)

Kolega (14) conducted a study of the oxygenation capacity of the model rotor used in experimental work reported in this thesis. This study related the oxygenation capacity to several rotor and channel parameters.

CHAPTER III

EXPERIMENTAL INVESTIGATION

Objectives

The objectives of this experimental investigation were:

1. Measurement of the velocity of liquid flowing in an oxidation ditch model at specified rotor and channel operating conditions
2. Measurement of the net power requirements for rotor operation at specified rotor and channel operating conditions
3. Determination of the effects changes in various rotor and channel parameters have on the mean liquid velocity in a channel
4. Determination of the effects changes in various rotor and channel parameters have on the net power requirements of the rotor
5. Partial verification of prediction equations developed for mean liquid velocity and rotor power requirements through use of data from a prototype oxidation ditch

Experimental Design

Conducting the experimental investigation as a model study offered the advantages of:

1. Construction expenses of a model were far below those of a prototype
2. Variation of rotor and channel parameters was simplified by use of a model study

As results of this investigation were intended to be applicable to prototype oxidation ditches, the design was carried out according to similitude principles, as given by Murphy (20).

Pertinent Quantities and Pi Terms

The quantities felt pertinent to investigation of mean liquid velocity are listed in Table II and illustrated in Figure 11.

The channel length and width are quantities defining the geometric size of the channel. The channel roughness index is a geometric characteristic defining the surface irregularities of the channel (20).

Liquid depth is measured as the depth of liquid above the main channel floor, measured under quiescent conditions at the point of velocity measurement. The liquid physical properties pertinent to this study are liquid density and viscosity. These properties allow evaluation of Reynold's numbers for both the ditch and the rotor.

Rotor diameter, rotor width, and paddle finger width are geometric quantities characterizing the rotor being used. Rotor width is the total width of one paddle blade, while paddle finger width is the width of the individual teeth composing one blade.

Rotor speed and paddle immersion depth define the rotor operating conditions. Paddle immersion depth is defined as the maximum depth of immersion a paddle blade undergoes as it rotates through the liquid, measured under quiescent liquid conditions.

TABLE II

PERTINENT QUANTITIES FOR MEAN LIQUID VELOCITY

No	Symbol	Description	Units	Dimensional Symbol
1	V	Mean velocity of liquid flow	ft/sec	L/T
2	d	Liquid depth	ft	L
3	e	Channel roughness index	ft/ft	-
4	W_c	Channel width	ft	L
5	L_c	Channel length	ft	L
6	ρ	Liquid mass density	lb_m/ft^3	M/L^3
7	μ	Liquid absolute viscosity	lb_f-sec/ft^2	FT/L^2
8	P_{id}	Paddle immersion depth	ft	L
9	W_r	Rotor width	ft	L
10	D	Rotor diameter	ft	L
11	P_w	Paddle finger width	ft	L
12	n	Rotor speed	rev/sec	1/T
13	G	Gravitational effect	lb_f/lb_m	F/M
14	Ne	Newton's Second Law Coefficient	lb_f-sec^2/lb_m-ft	FT^2/ML

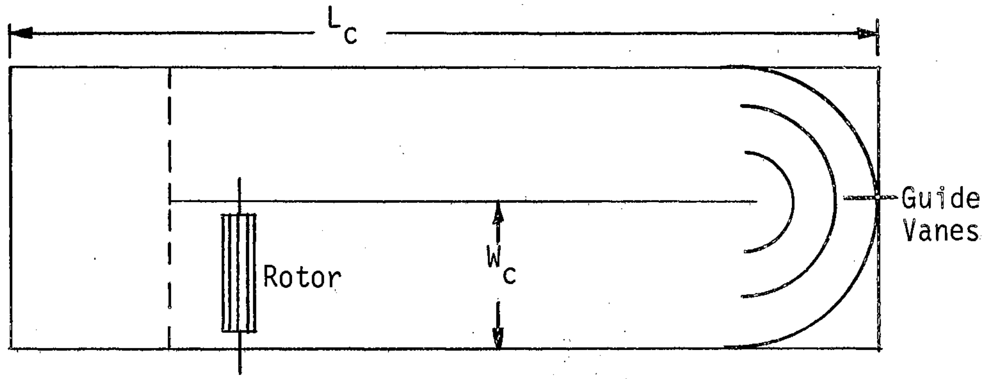

TOP VIEW OF DITCH MODEL

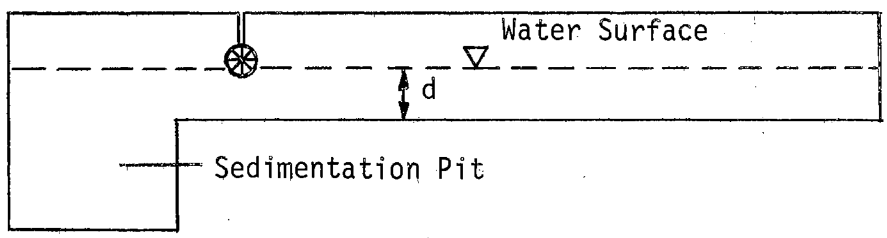

SIDE VIEW OF DITCH MODEL

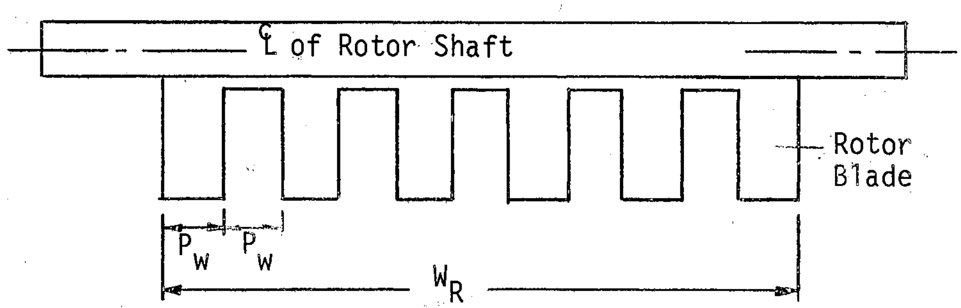

SIDE VIEW OF ROTOR BLADE

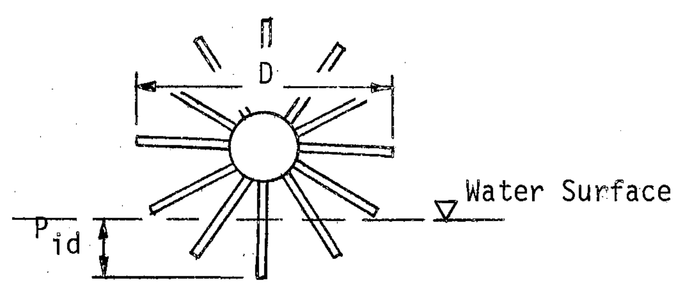

END VIEW OF ROTOR

Figure 11. Illustration of Pertinent Quantities.

The pertinent quantities were combined according to the Buckingham Pi Theorem to form the dimensionless parameters listed in Table III.

The quantities felt pertinent to investigation of net rotor power requirements are listed in Table IV.

Comparison of this set of quantities with the pertinent quantities listed for mean liquid velocity reveals the only new quantity to be that of net power required for rotor operation, which replaces the mean velocity term in the previous set.

The Buckingham Pi Theorem was again used to form the dimensionless parameters listed in Table V.

Comparison of the two sets of pi terms formed reveals the two sets are identical except for the dependent pi term. This model design allows investigation of both mean liquid velocity and rotor power requirements under the same testing schedule, thereby simplifying the investigation somewhat.

Selection of Values of Independent Pi Terms

The model used in conducting the experimental investigation was built such that the length scale of prototype length to model length was 12. All geometric elements of the channel and rotor were scaled by this ratio.

To simplify model design, the terms pi_8, pi_9, and pi_{10} were held at constant values throughout the experimental investigation.

A ratio of rotor width to channel width ($pi_8 = \frac{W_r}{W_c}$) as near unity as practical would minimize recirculation of water through the rotor without first flowing around the ditch. For the model, pi_8 was held at a value of 0.798 by use of a rotor width of 5.5 inches and a channel width of 6.9 inches.

TABLE III

DIMENSIONLESS PARAMETERS FOR MEAN LIQUID VELOCITY

No	Term	Description	Values
pi_1	$\frac{V^2\ Ne}{G\ d}$	Froude number for ditch	Dependent
pi_2	$\frac{Ne\ D\ n^2}{G}$	Froude number for rotor	Variable
pi_3	$\frac{Ne\ \rho\ D^2\ n}{\mu}$	Reynold's number for rotor	Variable
pi_4	$\frac{P_w}{D}$	Paddle finger width to rotor diameter ratio	Variable
pi_5	$\frac{P_{id}}{D}$	Paddle immersion depth to rotor diameter ratio	Variable
pi_6	$\frac{D}{d}$	Rotor diameter to liquid depth ratio	Variable
pi_7	$\frac{W_c}{L_c}$	Channel width to channel length ratio	Variable
pi_8	$\frac{W_r}{W_c}$	Rotor width to channel width ratio	Constant
pi_9	$\frac{D}{W_r}$	Rotor diameter to rotor width ratio	Constant
pi_{10}	e	Channel surface roughness index	Constant

TABLE IV

PERTINENT QUANTITIES FOR NET ROTOR POWER REQUIREMENTS

No	Symbol	Description	Units	Dimensional Symbol
1	P	Net power required for rotor operation	ft-lb_f/sec	LF/T
2	d	Liquid depth	ft	L
3	e	Channel roughness index	ft/ft	-
4	W_c	Channel width	ft	L
5	L_c	Channel length	ft	L
6	ρ	Liquid mass density	lb_m/ft^3	M/L^3
7	μ	Liquid absolute viscosity	lb_f-sec/ft^2	FT/L^2
8	P_{id}	Paddle immersion depth	ft	L
9	W_r	Rotor width	ft	L
10	D	Rotor diameter	ft	L
11	P_w	Paddle finger width	ft	L
12	n	Rotor speed	rev/sec	1/T
13	G	Gravitational effect	lb_f/lb_m	F/M
14	Ne	Newton's Second Law Coefficient	lb_f-sec^2/lb_m-ft	FT^2/ML

TABLE V

DIMENSIONLESS PARAMETERS FOR NET ROTOR POWER REQUIREMENTS

No	Term	Description	Values
pi_1	$\frac{P}{\rho\ n^3\ D^5\ Ne}$	Rotor power parameter	Dependent
pi_2	$\frac{Ne\ D\ n^2}{G}$	Froude number for rotor	Variable
pi_3	$\frac{Ne\ \rho\ D^2\ n}{\mu}$	Reynold's number for rotor	Variable
pi_4	$\frac{P_w}{D}$	Paddle finger width to rotor diameter ratio	Variable
pi_5	$\frac{P_{id}}{D}$	Paddle immersion depth to rotor diameter ratio	Variable
pi_6	$\frac{D}{d}$	Rotor diameter to liquid depth ratio	Variable
pi_7	$\frac{W_c}{L_c}$	Channel width to channel length ratio	Variable
pi_8	$\frac{W_r}{W_c}$	Rotor width to channel width ratio	Constant
pi_9	$\frac{D}{W_r}$	Rotor diameter to rotor width ratio	Constant
pi_{10}	e	Channel surface roughness index	Constant

The term pi_9 $(\frac{D}{W_r})$ was held constant at a value of 0.409, using a model rotor diameter of 2.25 inches.

Channel lengths used in the model were 40, 47.5, 55, 62.5, and 70 inches, resulting in pi_7 $(\frac{W_c}{L_c})$ values of 0.173, 0.145, 0.125, 0.110, and 0.099 respectively.

Liquid depths used ranged from 1 to 5 inches, corresponding to prototype depths of from 1 to 5 feet respectively.

Paddle immersion depths of from 1/8 to 5/8 inch were chosen, corresponding to prototype immersions of from 1.5 to 7.5 inches. Paddle finger widths of 0.156, 0.250, and 0.500 inches were used.

Analysis of terms pi_2 $(\frac{Ne\ D\ n^2}{G})$ and pi_3 $(\frac{Ne\ \rho\ D^2\ n}{\mu})$ yielded the following requirements for model to prototype rotor speed, respectively:

$$pi_2: \quad n_m = 3.46\ n_p$$

$$pi_3: \quad n_m = 144\ \frac{\rho_p\ \mu_m}{\rho_m\ \mu_p}\ n_p$$

where the subscripts m denotes the model and p denotes the prototype. Satisfaction of both requirements would require use of a fluid possessing a kinematic viscosity approximately equal to 0.024 times the kinematic viscosity of effluent found in a prototype ditch. As effluent in a prototype may be expected to exhibit properties very similar to those of water (due to high dilution with water), it proved impractical to satisfy both pi_2 and pi_3 speed ratio requirements.

Model rotor speeds of from 100 rpm (revolutions per minute) to 500 rpm were selected, based on the pi_2 speed ratio. It was theorized that use of speeds based on pi_3, (assuming equal model and prototype kinematic viscosities) would introduce appreciable error into the investigation due to windage effects on the rotor.

Due to the relatively large volume of liquid required in the model, it was felt most practical to select water as the fluid used in the model.

<u>Dependent Pi Term Selection</u>

In selection of the pi terms used in the experimental design, use of a Reynold's number for the ditch ($\frac{V\ d\ \rho\ Ne}{\mu}$) as the dependent pi term was considered. This term was rejected, however, and the Froude number of the rotor ($\frac{V^2\ Ne}{G\ d}$) selected as the dependent pi term after analyzing the relationship between model and prototype rotor blade tip velocities and the predicted relationship between model and prototype mean liquid velocities.

Since the model size is 1/12 prototype size and model rotation speed is $\sqrt{12}$ times prototype rotation speed, the model rotor blade tip velocity is $\frac{1}{\sqrt{12}}$ that found in a prototype.

This relationship is similar to the predicted relationship between model and prototype mean liquid velocities using the Froude number for the ditch as the dependent term. This relationship is:

$$V_m = \frac{1}{\sqrt{12}} V_p$$

However, if Reynold's number were used, the predicted relationship between mean liquid velocity in the model and prototype would be (assuming approximately equal viscosities in the model and prototype):

$$V_m = 12\ V_p$$

Thus, assuming that mean liquid velocity is related to rotor blade tip velocity, the Froude number for the ditch was selected as the dependent pi term.

Testing Schedule

Ideally, a schedule of tests would vary each independent pi term through its selected range of values while holding the other independent terms constant. This procedure was used in evaluation of the independent terms pi_4, pi_5, pi_6, and pi_7; but, it proved more practical to evaluate the terms pi_2 and pi_3 jointly rather than independently.

The testing schedule is given in Table VI.

TABLE VI

EXPERIMENTAL TESTING SCHEDULE

Run No	Pi_2 & Pi_3	Pi_4	Pi_5	Pi_6	Pi_7
1-5	Rotor speeds of 100, 200, 300, 400, & 500 rpm	Paddle finger width of 0.156 inch*	Immersion depth of 3/8 inch*	Liquid depth of 3 inches*	Tank length of 70 inches*
6-7	Rotor speed of 300 rpm*	Paddle finger widths of 0.250 and 0.500 inches	↓	↓	↓
8-11	↓	Paddle finger width of 0.156 inch	Immersion depths of 1/8, 1/4, 1/2, & 5/8 inch	↓	↓
12-15	↓	↓	Immersion depth of 3/8 inch	Liquid depths of 1, 2, 4, & 5 inches	↓
16-19	↓	↓	↓	Liquid depth of 3 inches	Tank lengths of 40, 47.5, 55, and 62.5 inches

*Initial model operating values

CHAPTER IV

EQUIPMENT

Oxidation Ditch Model

Similitude principles were used in designing the oxidation ditch model to be geometrically similar to a possible prototype. Design of model components was based on two prototype ditches. These were the oxidation ditch built at the Iowa State University Swine Nutrition Farm at Ames, Iowa, and the oxidation ditch now being constructed under the caged cattle building at the Oklahoma State Agricultural Experiment Station Farm at Stillwater, Oklahoma. As a length scale of 12 was used, a model dimension of one inch corresponded to a prototype length of one foot.

Requirements for the material from which the model was constructed were that it must be capable of supporting the direct attachment of the rotor mounts and must possess a characteristic surface roughness modeling that of a concrete prototype. One-half-inch plexiglass was used to construct the model, which was built by shop personnel in the Agricultural Engineering Department.

The model used in the experimental research consisted of a shallow rectangular tank with a sedimentation pit at one end. The shallow tank was divided into two channels by a partition of adjustable length. A plan of the model is given in Figure 12 and the model is shown in Figure 13.

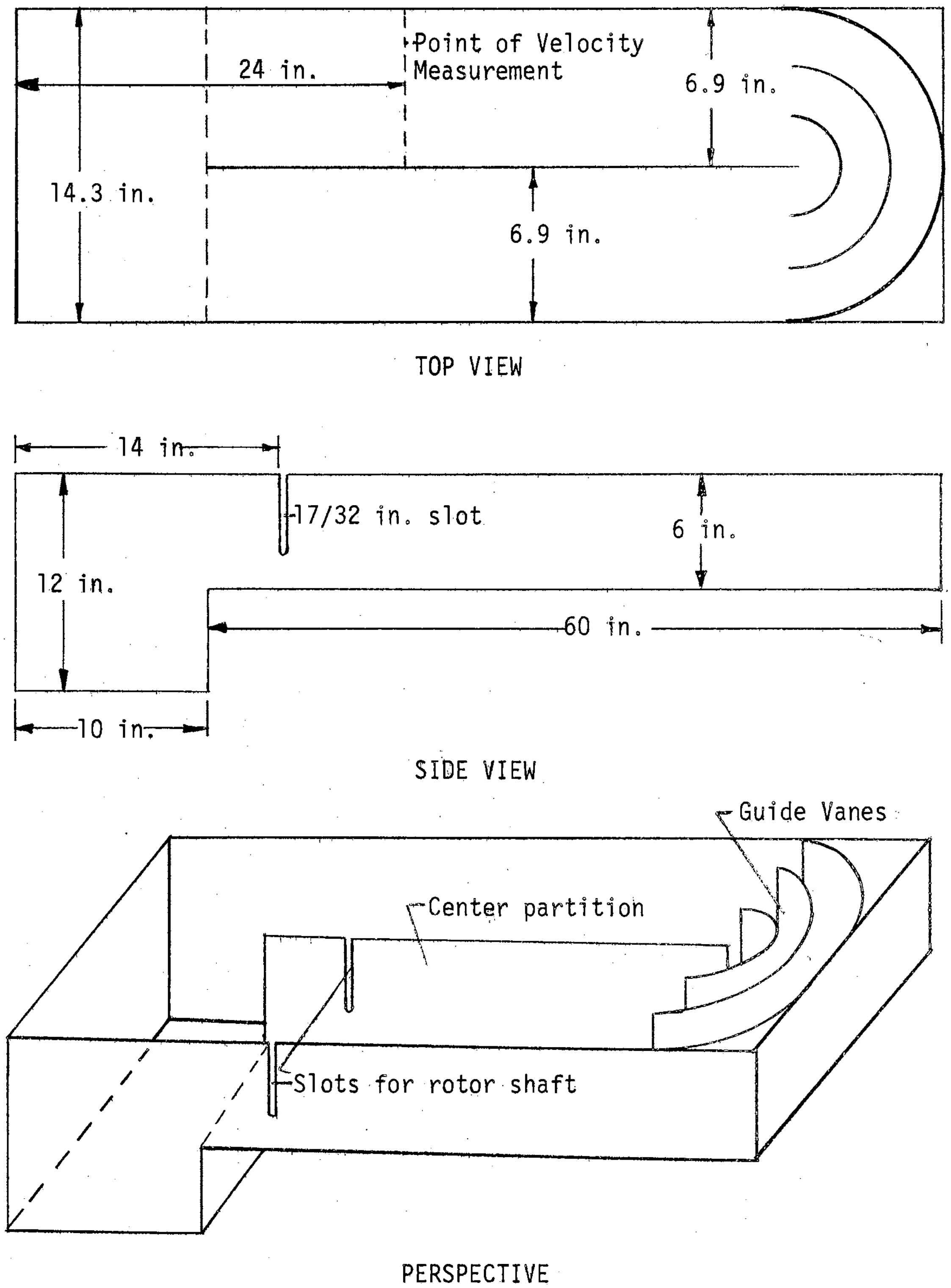

Figure 12. Oxidation Ditch Model.

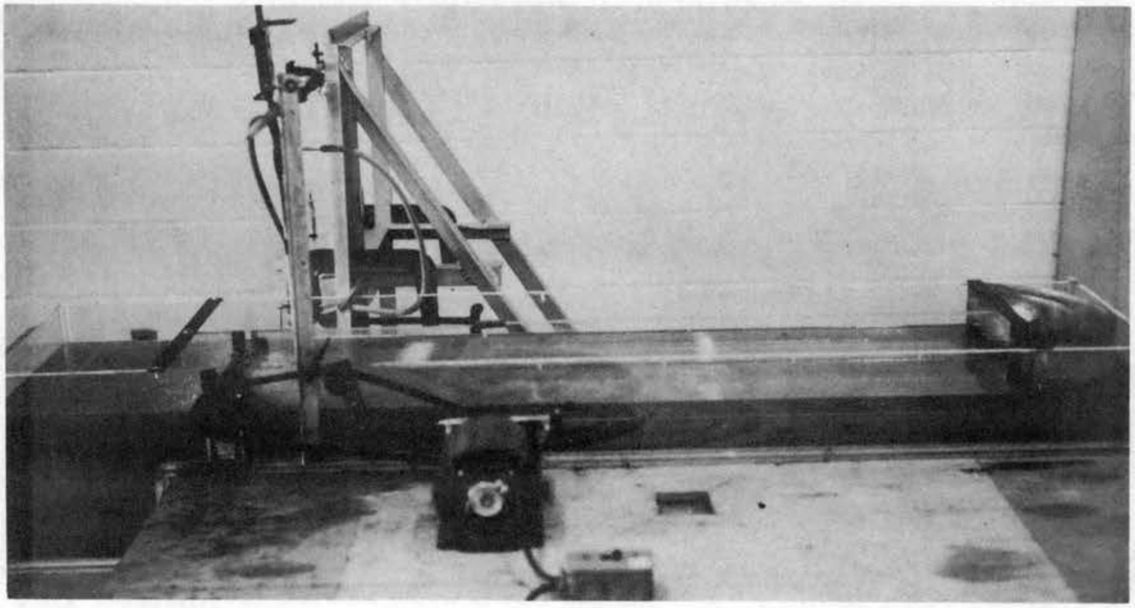

Figure 13. General View of Oxidation Ditch Model Showing All Components.

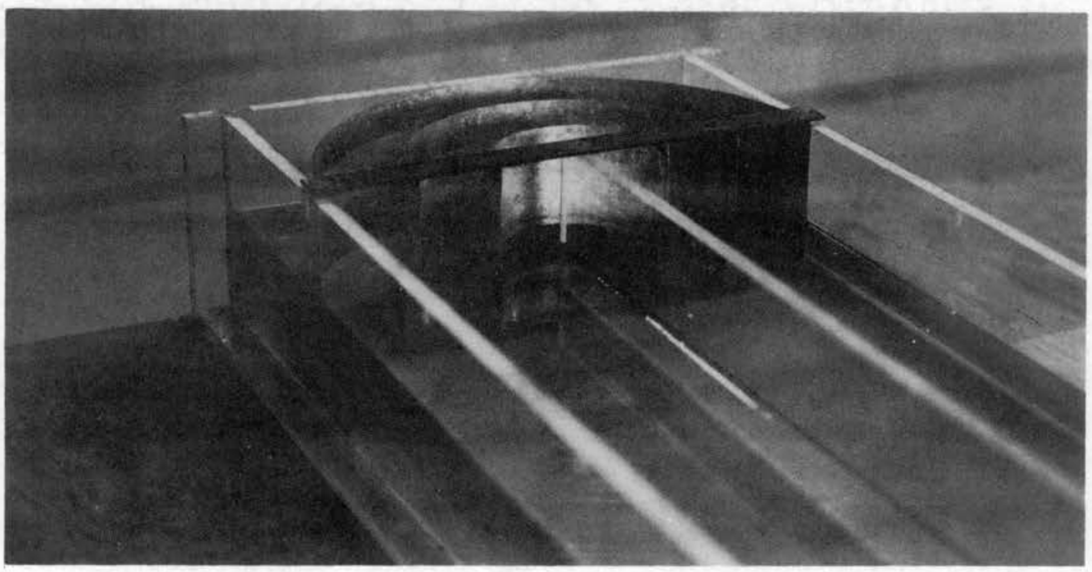

Figure 14. Guide Vanes Installed in Ditch.

Sheet metal guide vanes, shown in Figure 14, were installed in the model at the end opposite the sedimentation pit to increase the uniformity of velocity occurring across the channel section at the point of velocity measurement. While guide vanes would probably not be used in a prototype oxidation ditch, it was felt that including them in the model would increase the accuracy of velocity measurement by increasing the uniformity of flow.

The center partition was installed in two sections. A 20-inch section was permanently fixed to the tank bottom and used for mounting the rotor. The other section was connected to the fixed section by brackets, and was also connected to the metal guide vanes. Tank length was decreased by shortening this section and moving the guide vanes to correspond to the shorter tank length.

The model was fastened to a rigid table anchored to the lab floor with brackets, thus reducing vibration of the model.

Aeration Rotor Model

The rotor used in the experimental research was designed and used previously by Kolega (14) in work on determination of the oxygen transfer coefficient of aeration rotors. A length scale of 12 was used in modeling the rotor, using as a prototype the 27.5-inch diameter cage rotor manufactured by Lakeside Engineering Company of Chicago, Illinois. A plan of the rotor is given in Figure 15, and a detailed plan is available from the Oklahoma State University Agricultural Engineering Department as drawing number C-211.

The rotor was mounted in the channel 14 inches from the end of the sedimentation pit and is shown in Figure 16. Stove bolts were used for fastening the rotor mounts to the sides of the channel.

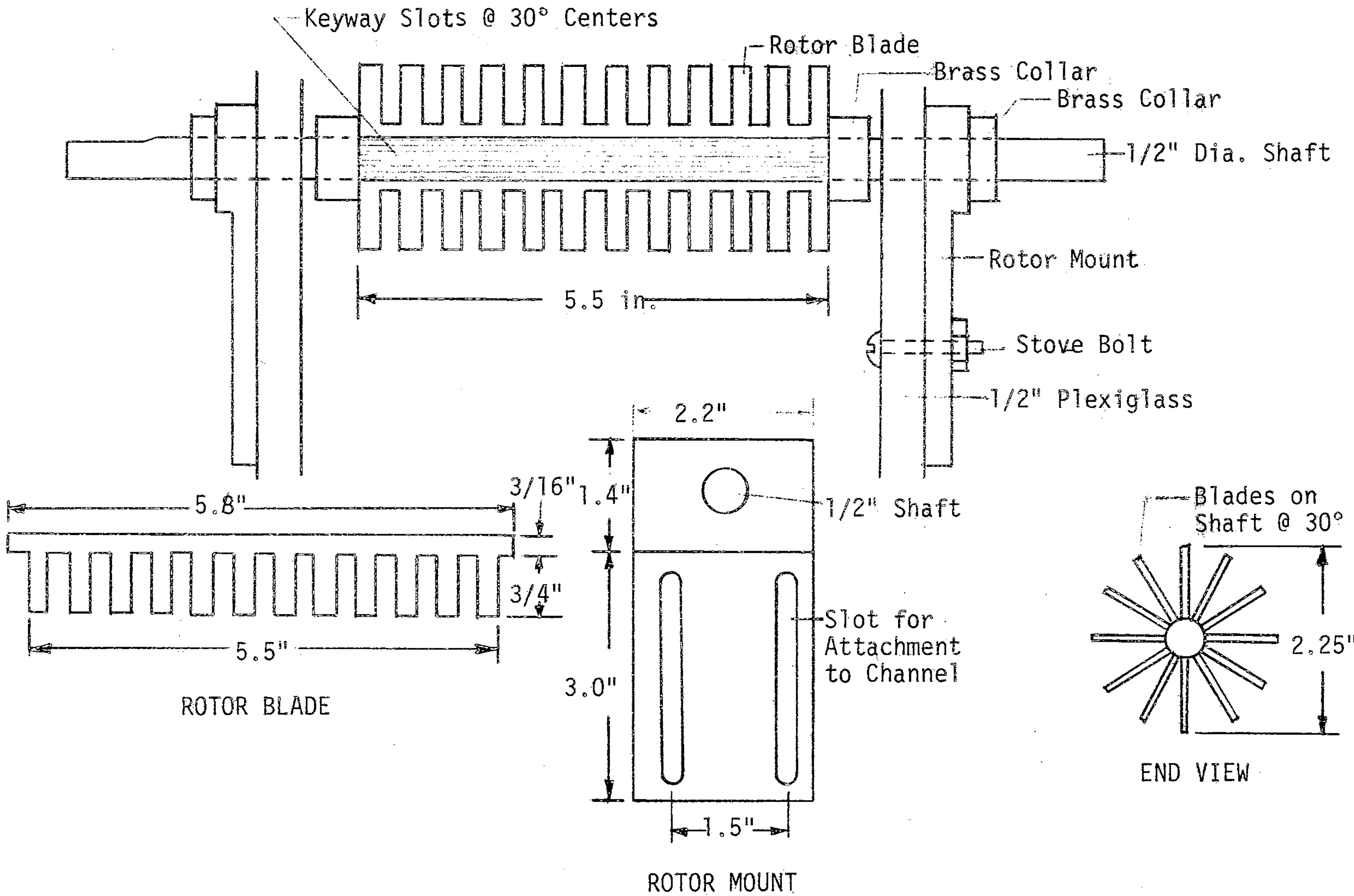

Figure 15. Details of Rotor and Rotor Mounts.

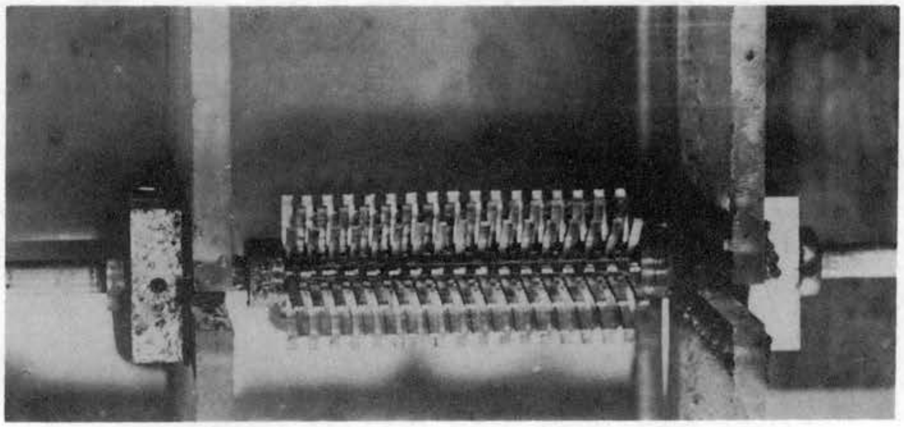

Figure 16. Top View of Aeration Rotor Installed in Ditch.

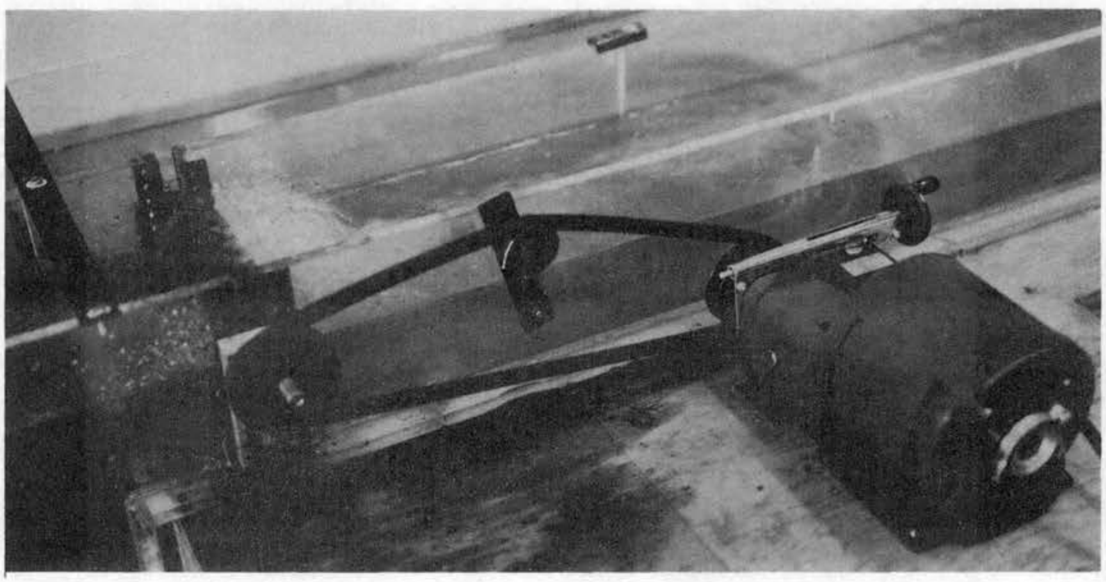

Figure 17. View of Drive Assembly and Rotor in Operation.

The rotor was driven by a Zero-Max E2-M2 mechanical variable speed drive unit, manufactured by the Zero-Max Company of Minneapolis, Minnesota. The unit consisted of a 1/6 horsepower motor operating at 1800 rpm and a speed reduction unit capable of delivering a constant torque of up to 12 inch-pounds at output shaft speeds of from 0 to 400 rpm.

The drive unit was fastened to the table on which the ditch model was mounted, and a V-belt was used to connect the drive unit and rotor, as shown in Figure 17. Belt tension was controlled by a small pulley bolted to the side of the ditch.

Velocity Measuring Equipment

The flow velocity of the liquid in the model was measured by use of a Dwyer #160 pitot-static tube of 5/16-inch outside diameter, manufactured by the F. W. Dwyer Manufacturing Company of Michigan City, Indiana.

As relatively small velocities were obtained in operating the model (most velocity measurements were less than 0.5 fps, corresponding to velocity heads of less than 0.047 inches of water), the velocity measuring apparatus had to be capable of measuring small water level differences.

The arrangement shown in Figures 18, 19, and 20 was used to measure flow velocities in the model. The pitot-static tube was connected to an inverted Dwyer #1420 hook gage manometer with two short lengths of vacuum tubing. Hook gage micrometers were used to measure the liquid level in the manometer cells, and were capable of measuring depths to within 0.001 inch. The inverted manometer was clamped to a metal stand

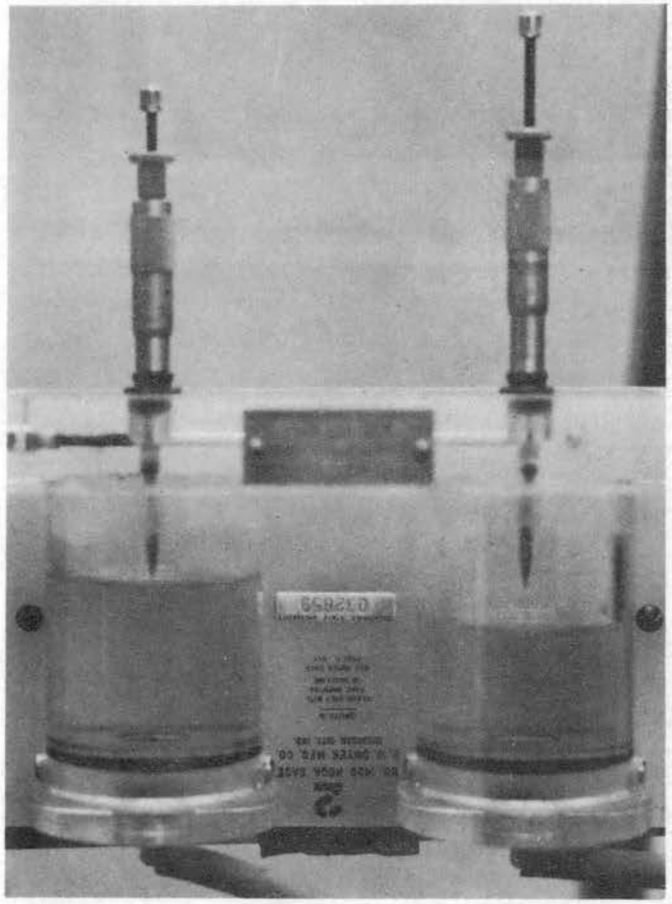

Figure 18. Hook Gage Manometer in Inverted Position.

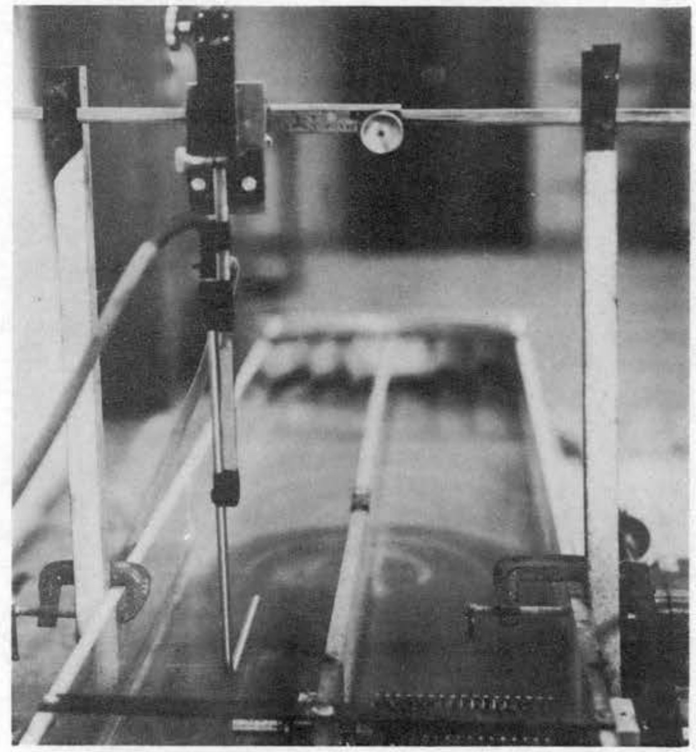

Figure 19. Pitot-Static Tube and Positioning Apparatus

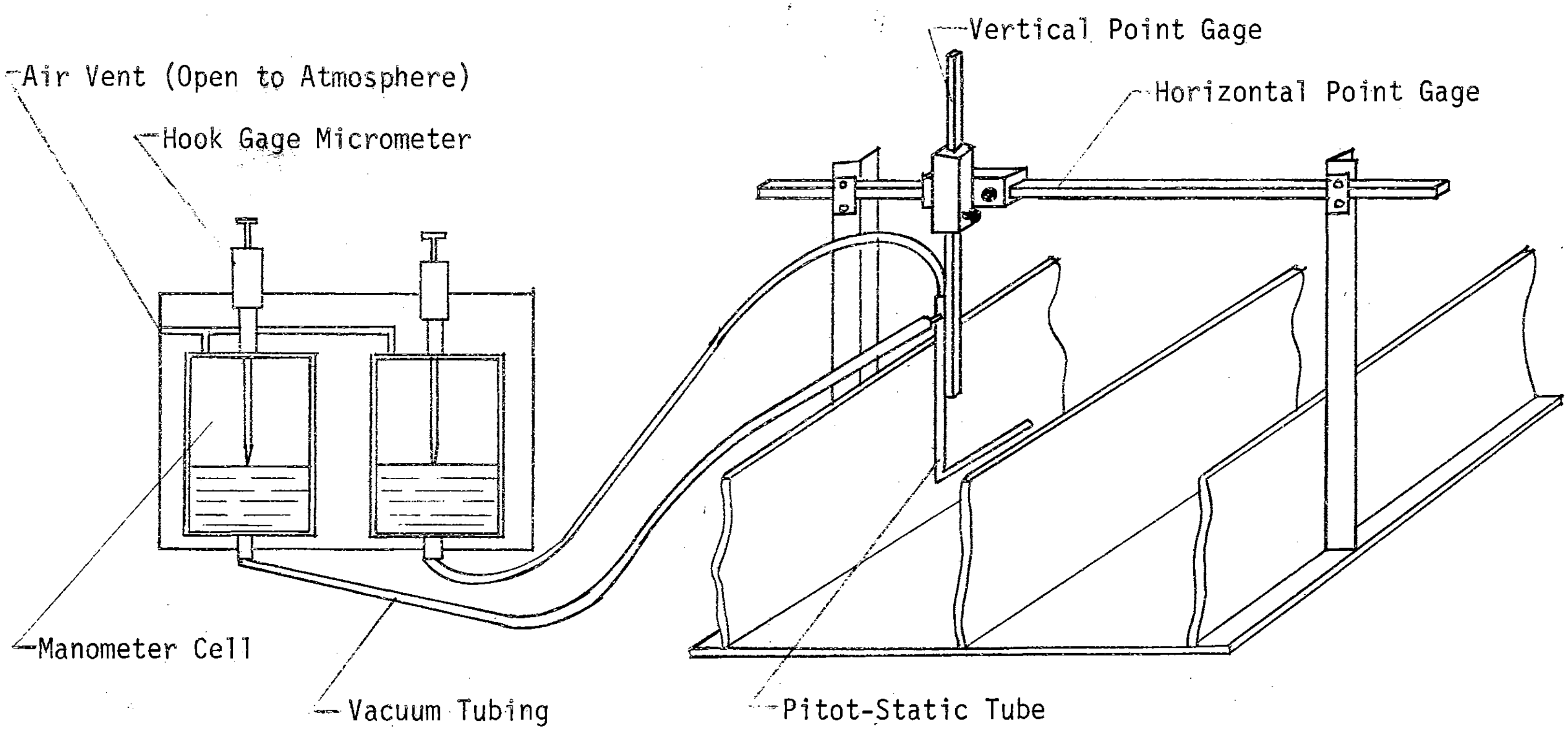

Figure 20. Illustration of Velocity Measuring Apparatus.

bolted to the shop floor, to protect against accidental movement of the apparatus during a test.

Water was used as the pressure transferring medium for the system. This was accomplished by placing the manometer at the level of the water surface in the ditch and replacing the air in the pitot-static tube and vacuum tubing with water. Under quiescent conditions the water levels in the manometer cells and in the model ditch were at the same elevation, due to the siphon effect of the system.

Determination of the mean flow velocity in the channel required making vertical traverses of the liquid with the pitot-static tube at several positions across the width of the channel. To facilitate making these traverses, the arrangement shown in Figure 19 and illustrated in Figure 20 was used. Two structural steel angle iron sections 2 feet long were clamped in a vertical position to the outside edges of the model. A point gage with a 2-foot range and manufactured by Fred Lory, Jr., of Davis, California, was fastened in a horizontal position to the vertical angle iron sections at a height 22 inches above the channel bottom. Another point gage was attached vertically to the adjustment mechanism of the horizontal gage, and the pitot-static tube was fastened to the vertical gage. Using this arrangement, positions across the channel width were controlled by adjusting the horizontal point gage, while vertical positioning was accomplished by adjustment of the vertical gage.

CHAPTER V

EXPERIMENTAL PROCEDURE

Velocity measurements were made in the channel not containing the rotor at a position 24 inches from the end of the sedimentation pit. This position was chosen since the flow was more uniform in this area than in other areas and since no surface protrusions existed immediately upstream from this position.

Preliminary Investigation

In determining the procedure to follow in running the tests, several preliminary tests were performed.

As velocity head readings were obtained in manometer cells of large surface area (cell inside diameter was 2.5 inches), an increase in the water level in the cells required the movement of a relatively large quantity of water through the tubing to the cells. Thus, the time required for stabilization of the water level in the cells was dependent on the magnitude of the change in water level of the cells.

Tests were run to determine the time interval required between velocity measurements to assure that stabilization of water level had occurred. For these tests the various operating parameters were set at the values specified in the experimental design as the initial model operating values. The rotor was first operated for an hour to assure that the system was completely stabilized. The pitot-static tube position in the liquid was then set at a new level and water level readings taken in the manometer cells at 5-minute intervals until 20 minutes had elapsed. This procedure was repeated until 5 sets of readings had been obtained. Comparison of readings showed no appreciable differences (within the accuracy of measurement possible) between the readings taken at 5 and 20 minutes elapsed time. Similar tests for periods less than 5 minutes indicated that 5 minutes was probably the minimum interval which would assure that water level stabilization had occurred.

Tests were also conducted to determine the difference in mean velocity values obtained for a test run by making 3 and 5 vertical traverses of the liquid depth. The channel was divided into either 3 or 5 sections of equal width, and vertical velocity traverses were made at the center-line of each section. Readings were taken at 1/3-inch depth increments, and the mean velocity for each method was computed. Comparison of results indicated the mean velocity values were within 5 percent of each other. Since the time required for a test run was greater if 5 vertical traverses were made, the tests were conducted taking 3 vertical traverses per test.

Testing Procedure

The following procedure was used in collecting data for determination of mean liquid velocity:

1. The operating parameters were set at their specified values for each test run and these values recorded, along with liquid temperature and room barometric pressure.
2. The pitot-static tube was set at the first velocity measurement position in the channel, with this position

being 1/6 inch above the bottom of the center-line of the channel.

3. The pitot-static tube and vacuum tubing were "bled" to remove all air from the lines.

4. The liquid level in the manometer cells was allowed to stabilize under quiescent conditions (rotor not operating) for one hour and then read. These levels were recorded as initial static and total head readings.

5. The rotor was operated for one-half hour to allow stabilization of liquid flow in the channel.

6. The channel was divided into 3 sections of equal width, and readings of static and total head were taken along the center-line of these sections. Velocity traverses were begun 1/6 inch above the channel bottom and proceeded vertically upward, with readings taken at 1/3-inch depth increments. The center section was traversed first, the outside section second, and the inside section last (inside section is one adjacent to center dividing partition). To assure that liquid level stabilization occurred in the manometer cells, readings were taken at 5-minute intervals.

7. For each measurement position the velocity head was found. Since the static water level changed during the testing period due to evaporation from the water surface and splashing from the channel at the rotor,

it was necessary to correct the total head reading to reflect this static level change. This was done by computing the decrease in static level from its initial level and subtracting this amount from the initial reading for total head. The velocity head for that measurement position was then found by subtracting this adjusted initial value for total head from the level reading obtained at that position during the test.

8. Velocity head measurements were converted to water velocities in feet per second, using the formula:

$$H = \frac{V^2}{2g}$$

where

H = water head in feet

V = water velocity in fps

g = acceleration of gravity--32.2 feet/sec^2

These velocity readings for each test are given in Appendix A.

9. The velocities for a vertical traverse were added and this sum divided by the number of readings in that traverse, yielding the arithmetic average velocity for the traverse. While it was recognized that other methods of determining the mean velocity existed (i.e., Simpson's Rule, use of planimeter to determine area under a velocity profile, etc.), it was not felt that the possible increase in accuracy which might

occur thru use of these methods was sufficiently large to justify the increased time required.

10. The average liquid velocity for a test run was computed by summing the average velocities for the traverses made in that test and dividing by the number of traverses made.

CHAPTER VI

VELOCITY MEASUREMENT RESULTS

Velocity traverses of the liquid were made at three positions across the channel width at a position 24 inches from the end of the sedimentation pit, following the method outlined in the experimental procedure. The velocity readings obtained are given in Appendix A.

As each traverse represented an equal width of channel, the mean liquid velocity for a test was found by first computing the arithmetic average velocity for each traverse and then determining the average of these values. Table VII gives a summary of the average velocities obtained. These results indicate that the mean liquid velocities found ranged from 0.178 fps to 0.523 fps. Average velocities at the outside measurement position were generally higher than at the center position, and velocities at the inside position were less than at the other positions for all tests.

Velocity profiles were drawn for each test, using the velocity readings given in Appendix A. The channel section which the profile represents is designated by using the notation ℄ for measurement of the center channel section, O for measurement of the outside section, and I for measurement of the inside channel section. Profiles were drawn as smooth curves and used the open channel flow assumption of zero velocity at the channel bottom.

TABLE VII

SUMMARY OF LIQUID VELOCITY TEST RESULTS

Run No.	Rotor Speed (rpm)	Finger Width (in)	Immersion (in)	Liquid Depth (in)	Tank Length (in)	Temp (°F)	Average Velocity in a Channel Section: Outside Section (fps)		Center Section (fps)		Inside Section (fps)	Mean Liquid Velocity (fps)
1	100	0.156	0.375	3.0	70	85	0.199		0.190		0.144	0.178
2	200	0.156	0.375	3.0	70	85	0.318		0.316		0.234	0.289
3	300	0.156	0.375	3.0	70	84	0.412		0.408		0.306	0.375
4	400	0.156	0.375	3.0	70	82	0.453		0.431		0.312	0.399
5	500	0.156	0.375	3.0	70	79	0.474		0.455		0.349	0.426
6	300	0.250	0.375	3.0	70	75	0.415		0.396		0.291	0.367
7	300	0.500	0.375	3.0	70	75	0.384		0.361		0.265	0.336
8	300	0.156	0.125	3.0	70	80	0.289		0.284		0.210	0.261
9	300	0.156	0.250	3.0	70	80	0.361		0.351		0.266	0.326
10	300	0.156	0.500	3.0	70	79	0.452		0.447		0.331	0.410
11	300	0.156	0.625	3.0	70	79	0.488		0.460		0.338	0.429
12	300	0.156	0.375	1.0	70	75	0.589		0.546		0.433	0.523
13	300	0.156	0.375	2.0	70	75	0.460		0.481		0.349	0.430
14	300	0.156	0.375	4.0	70	78	0.328		0.305		0.227	0.287
15	300	0.156	0.375	5.0	70	79	0.315		0.285		0.227	0.276
16	300	0.156	0.375	3.0	62.5	72	0.393		0.386		0.269	0.349
17	300	0.156	0.375	3.0	55	72	0.406		0.425		0.258	0.363
18	300	0.156	0.375	3.0	47.5	73	0.425		0.459		0.411	0.432
19	300	0.156	0.375	3.0	40	73	0.466		0.478		0.079	0.341
20	300	0.156	0.375	3.0	40	81	0.373	0.659	0.502	0.257	0.054	0.369

Rotor Speed Test Results

Tests #1 thru 5 were conducted using rotor speeds of from 100 to 500 rpm in 100 rpm increments. Mean liquid velocity increased as rotor speed increased, which was the expected result. Observation indicated that increasing rotor speed also increased the quantity of water thrown up by the rotor and the number of water droplets formed. Velocity profiles for these tests are shown in Figure 21.

Paddle Finger Width Test Results

Paddle finger widths of 0.156, 0.250, and 0.500 inches were tested in tests #3, 6, and 7, respectively. Velocity profiles for these tests are given in Figure 22. Analysis of the results shows that mean liquid velocity increases with decreasing finger width. Little water was thrown up by the rotor when using the 0.500-inch finger width, and a small quantity of water was carried over the rotor and discharged into the channel opposite the direction of liquid flow. The 0.250-inch finger width rotor threw some water up as droplets, although the quantity thrown up was less than when the 0.156-inch finger width blade was used.

Paddle Immersion Depth Test Results

Paddle immersion depths of from 0.125 to 0.625 inches were tested in 0.125-inch increments in tests #3, 8, 9, 10, and 11. Analysis of results reveals that mean liquid velocity increased as immersion depth increased, which is the expected relationship. As shown on the velocity profiles in Figure 23, the highest velocities were found at the approximate center of the liquid depth. Observations indicated that

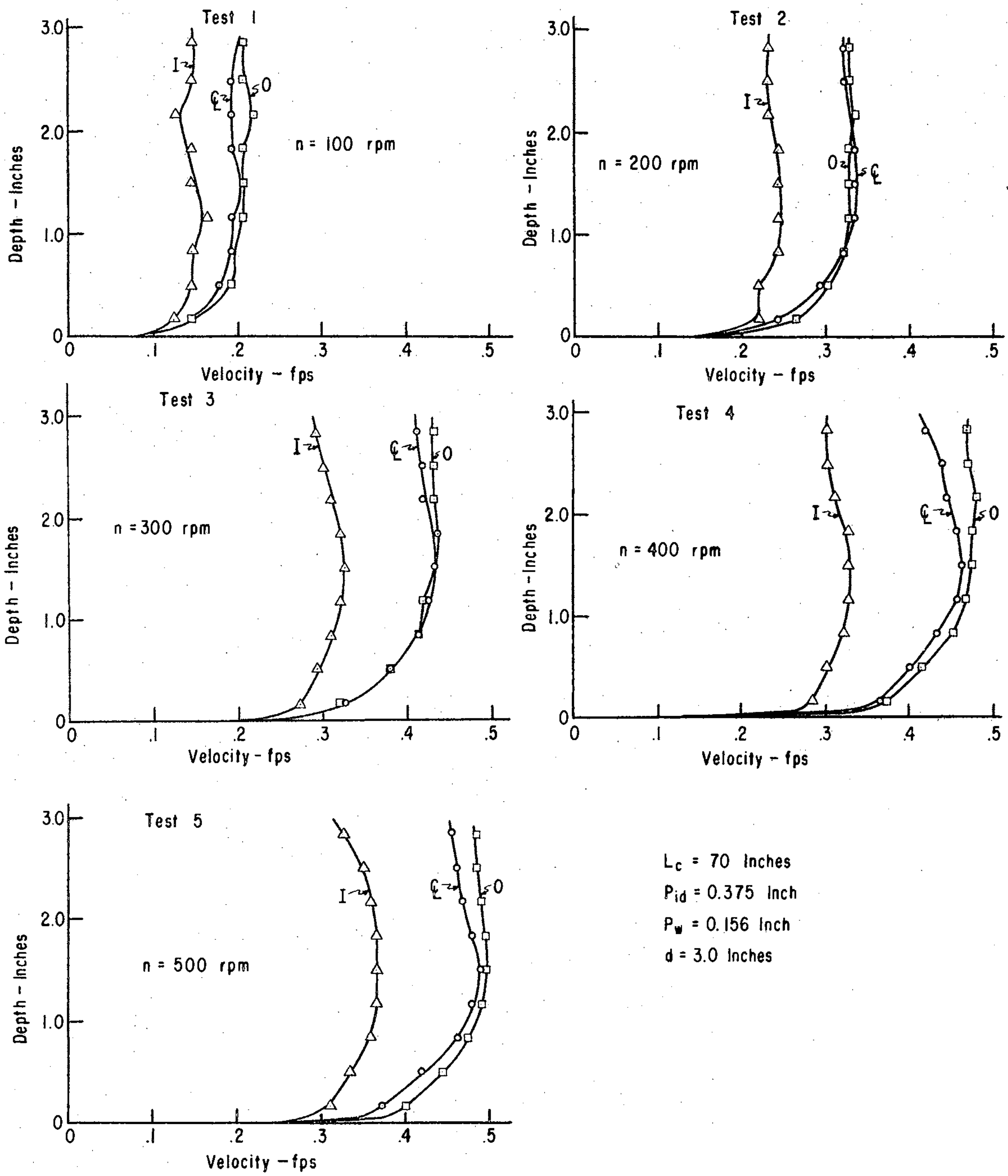

Figure 21. Velocity Profiles for Test Series Varying Rotor Speed.

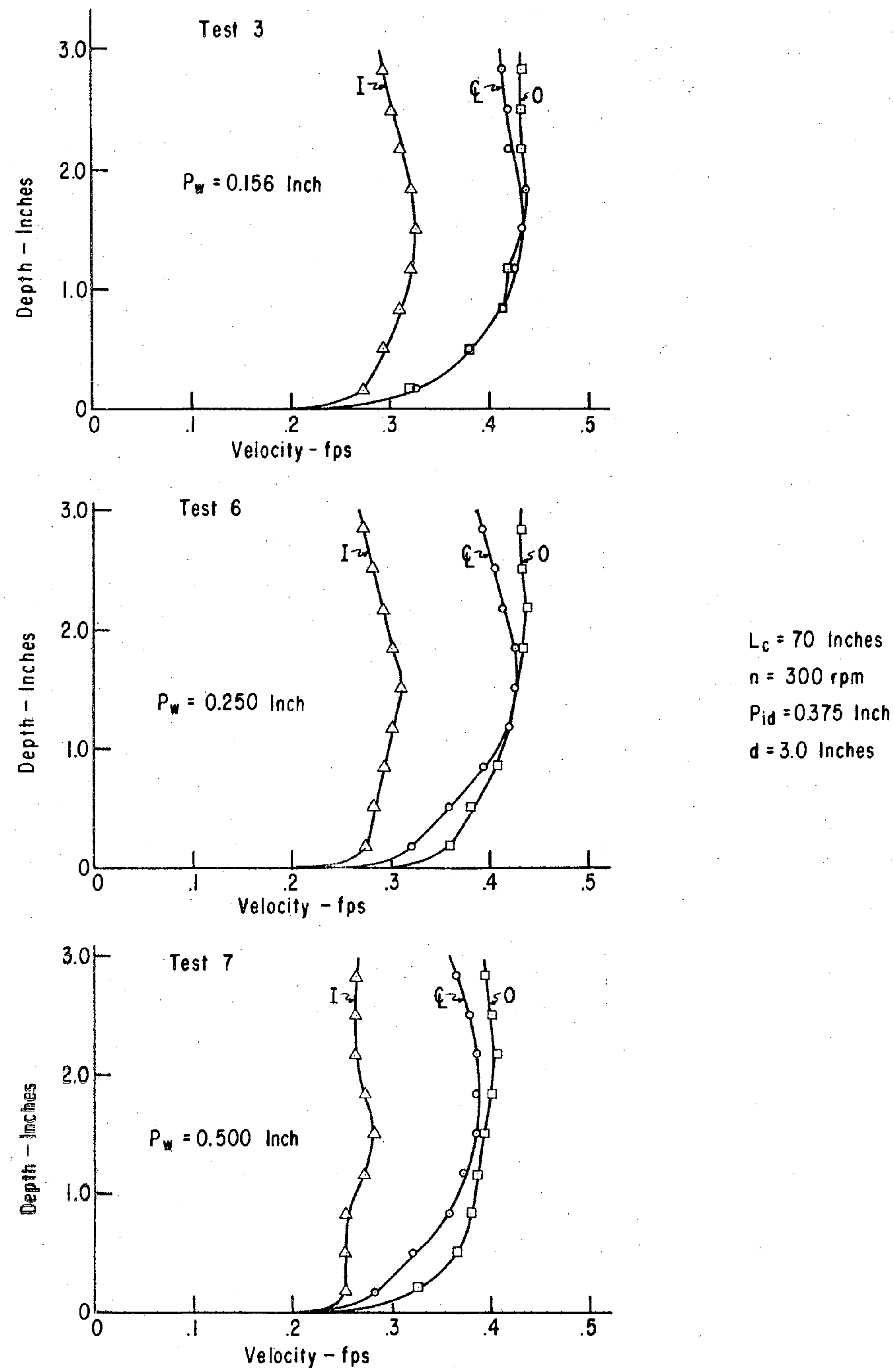

Figure 22. Velocity Profiles for Test Series Varying Paddle Finger Width.

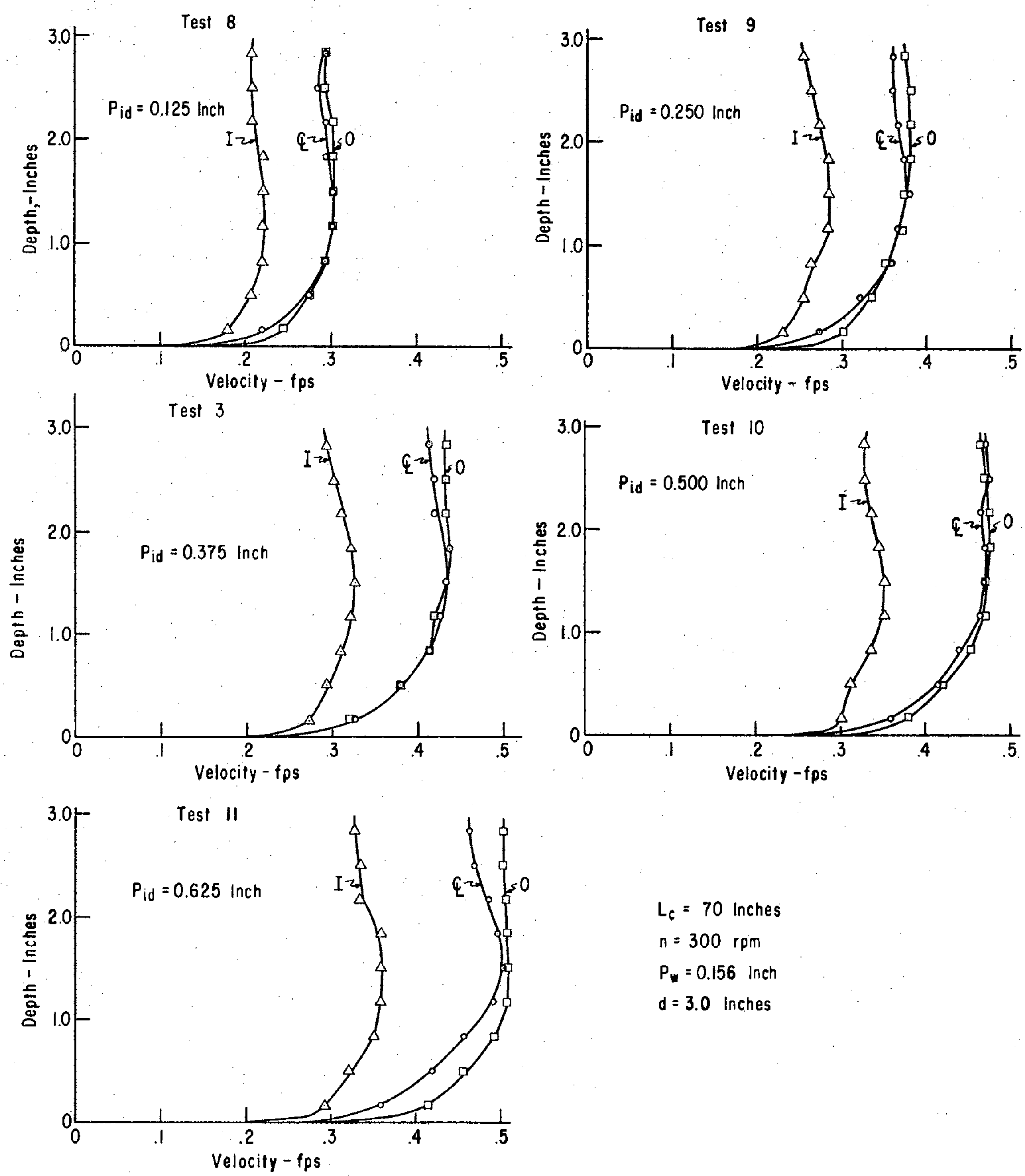

Figure 23. Velocity Profiles for Test Series Varying Paddle Immersion Depth.

the quantity of water thrown up at the rotor increased as the immersion depth increased.

Liquid Depth Test Results

Tests #3, 12, 13, 14, and 15 varied the liquid depth in the channel in one-inch increments, covering depths ranging from 1.0 inches to 5.0 inches. The mean liquid velocity increased as liquid depth decreased, while the observed water movement at the rotor did not change appreciably between tests. As shown on the velocity profiles in Figure 24, the highest velocities occurred at the water surface for the 1.0-inch liquid depth and moved downward relative to the liquid surface as liquid depth increased.

Channel Length Test Results

The channel length was changed in tests #3, 16, 17, 18, 19, and 20. Channel lengths of from 40 to 70 inches were tested, with velocity profiles for the tests given in Figure 25. The expected relationship was that mean velocity would increase as channel length decreased. However, test results failed to indicate clearly what effect changing the channel length had on the mean liquid velocity.

A possible explanation for the wide mean velocity differences found in this series of tests is that, as channel length decreased, the velocity distribution across the channel became less uniform and the velocity readings obtained became highly dependent on the position of velocity measurement. Thus, the velocity readings obtained may not have accurately reflected the true mean velocity in the channel. That the velocity readings were highly dependent on the position of measurement

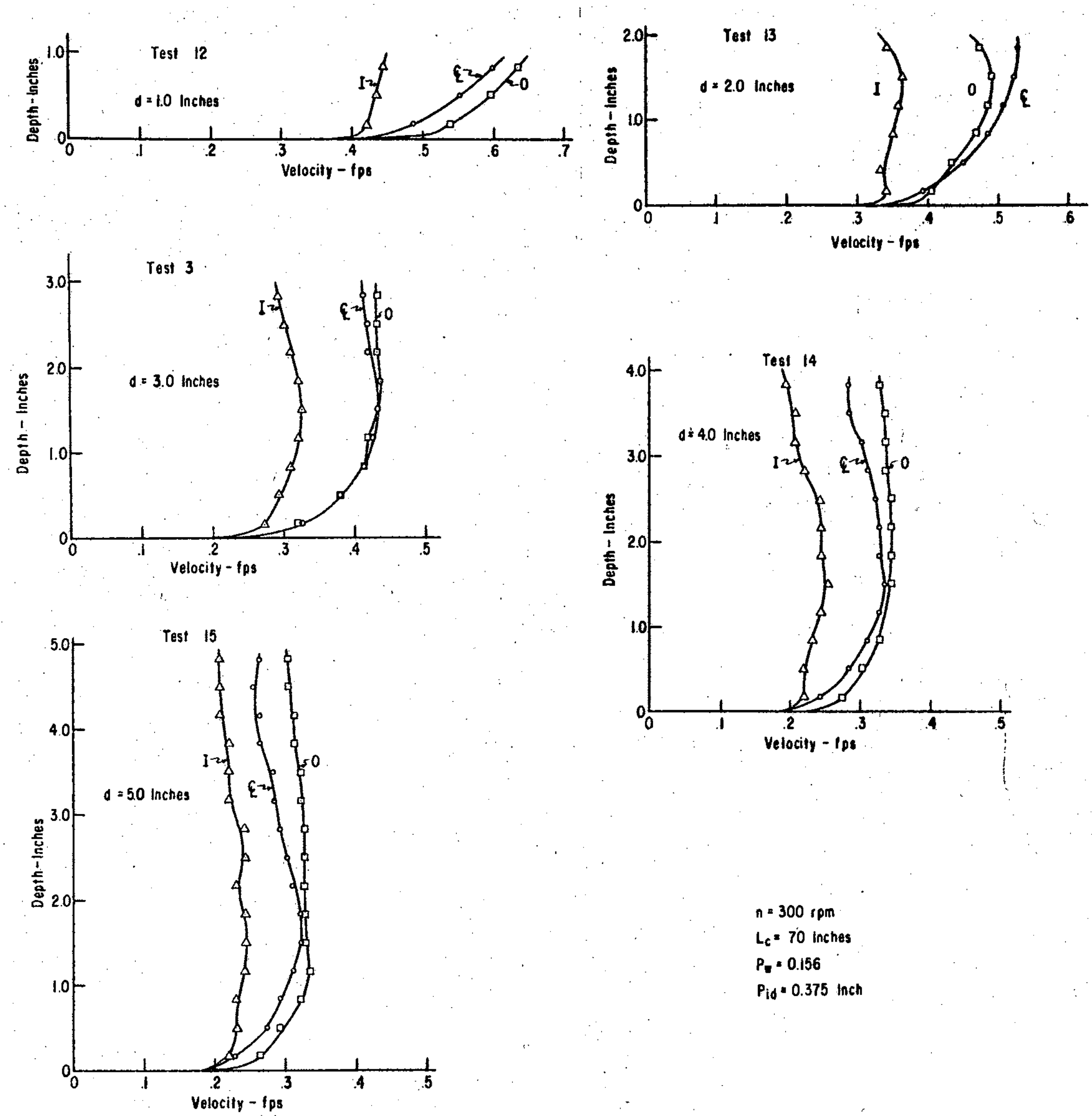

Figure 24. Velocity Profiles for Test Series Varying Liquid Depth in Channel.

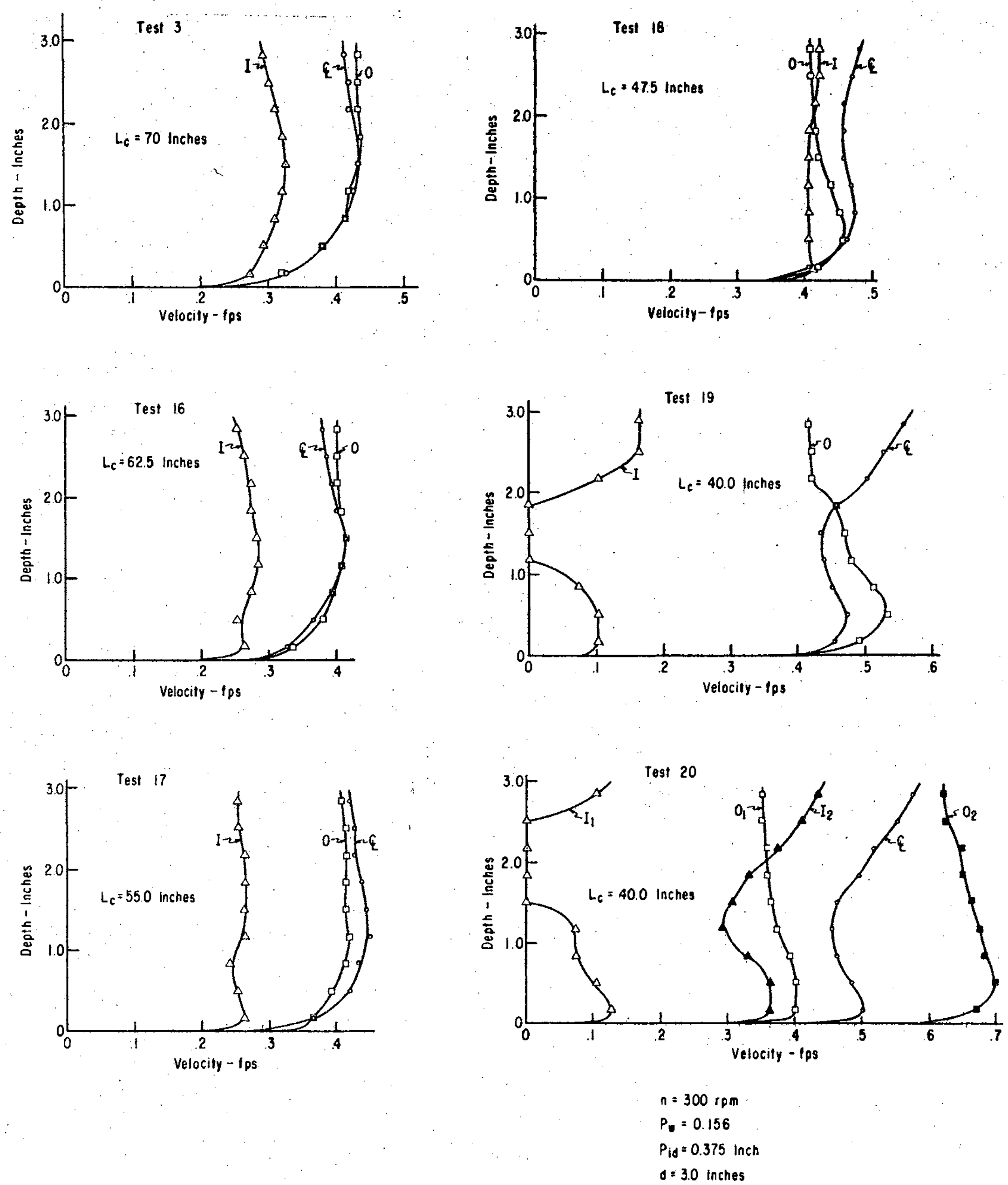

Figure 25. Velocity Profiles for Test Series Varying Channel Length.

can be seen by comparison of velocity profiles for tests #19 and 20. Both tests were conducted using a channel length of 40 inches, with three velocity traverses made in test #19 and five traverses made in test #20.

Also, some of the variation in mean liquid velocities found in this series of tests may be due to liquid viscosity differences that existed when the tests were conducted. Tests #16, 17, 18, and 19 were run at liquid temperatures of 72° F and 73° F, test #3 was run at 85° F, and test #20 was run at 81° F. If mean velocities were adjusted to compensate for the viscosity differences, the mean velocities of tests #3 and 20 would agree more closely with the mean velocities found for the other tests.

Observations on Sedimentation in Model

Limited observations were made on the sedimentation of small sand grains in the model. At low velocities sedimentation occurred throughout the model. Increasing the velocity caused most of the sand to be lifted from the bottom and carried in suspension by the liquid, although a small quantity of sand settled out on the channel floor immediately upstream from the sedimentation pit. At low velocities sedimentation occurred in the pit, but increasing the velocity caused this sediment to be lifted from the pit bottom and carried in suspension by the liquid.

CHAPTER VII

DATA ANALYSIS

An objective of this research was the development of a prediction equation relating mean liquid velocity in the channel to the independent pi terms investigated in the experimental study. This equation was developed by first determining component equations between the dependent pi term and each independent term and then combining these equations to form the prediction equation.

Values of the pi terms were computed for each test and listed in Table VIII.

Development of Component Equations

Pi_2 and Pi_3 Analysis

In conducting the experimental investigation, the independent terms pi_2 $(\frac{Ne\ D\ n^2}{G})$ and pi_3 $(\frac{Ne\ \rho\ D^2\ n}{\mu})$ were varied jointly, rather than investigating one term while holding the other constant. This procedure was followed since in conducting the investigation of these terms it proved practical to vary only rotor speed.

When values of the dependent term pi_1 $(\frac{V^2}{G}\frac{Ne}{d})$ were plotted against values of pi_2 on log-log paper, the plot appeared to be a straight line, as shown in Figure 26. The general form of the equation for such a relationship is:

TABLE VIII

VALUES OF PI TERMS IN EXPERIMENTAL INVESTIGATION

Test No.	Pi_1	Pi_2	Pi_3	Pi_4	Pi_5	Pi_6	Pi_7
1	0.00393	0.0162	6,688	0.0693	0.167	0.750	0.0986
2	0.0105	0.0648	13,376	0.0693	0.167	0.750	0.0986
3*	0.0175	0.1458	19,817	0.0693	0.167	0.750	0.0986
4	0.0197	0.2594	25,814	0.0693	0.167	0.750	0.0986
5	0.0227	0.4049	31,100	0.0693	0.167	0.750	0.0986
6	0.0158	0.1458	19,817	0.111	0.167	0.750	0.0986
7	0.0140	0.1458	19,817	0.222	0.167	0.750	0.0986
8	0.00845	0.1458	19,817	0.0693	0.058	0.750	0.0986
9	0.0131	0.1458	19,817	0.0693	0.120	0.750	0.0986
10	0.0210	0.1458	19,817	0.0693	0.218	0.750	0.0986
11	0.0228	0.1458	19,817	0.0693	0.280	0.750	0.0986
12	0.1011	0.1458	19,817	0.0693	0.167	2.228	0.0986
13	0.0337	0.1458	19,817	0.0693	0.167	1.098	0.0986
14	0.00769	0.1458	19,817	0.0693	0.167	0.563	0.0986
15	0.00567	0.1458	19,817	0.0693	0.167	0.449	0.0986
16	0.0152	0.1458	19,817	0.0693	0.167	0.750	0.1104
17	0.0163	0.1458	19,817	0.0693	0.167	0.750	0.1255
18	0.0231	0.1458	19,817	0.0693	0.167	0.750	0.1453
19	0.0144	0.1458	19,817	0.0693	0.167	0.750	0.1725
20	0.0169	0.1458	19,817	0.0693	0.167	0.750	0.1725

*Test at Initial Model Operating Values.

$$pi_1 = a\ (pi_2)^b$$

Values of the constant a and exponent b for this equation were found by a linear regression analysis performed by an IBM 7040 computer using Fortran IV Language. The equation computed for the relationship between pi_1 and pi_2 was:

$$pi_1 = 0.0428\ (pi_2)^{0.5526}$$

This equation gave a correlation coefficient between observed and computed pi_1 values of 0.982.

A plot of pi_1 against pi_3 also appeared as a straight line on log-log paper, as shown in Figure 27. An analysis similar to that carried out for pi_2 was conducted for pi_3, with the computed equation being:

$$pi_1 = 0.00000016\ (pi_3)^{1.1567}$$

The correlation coefficient for this equation was computed to be 0.987.

The above results indicate that either the pi_2 or the pi_3 equation could be used in development of the prediction equation. In this study the pi_2 equation was used, rather than the pi_3 equation. This choice was based on common practice followed when dealing with water in open channel flow; namely, the effect of viscosity is neglected (20).

Pi_4 Analysis

A plot of pi_1 against pi_4 $(\frac{P_w}{D})$ appeared to be a straight line on log-log paper, as shown in Figure 28. The equation computed for the relationship between pi_1 and pi_4 was:

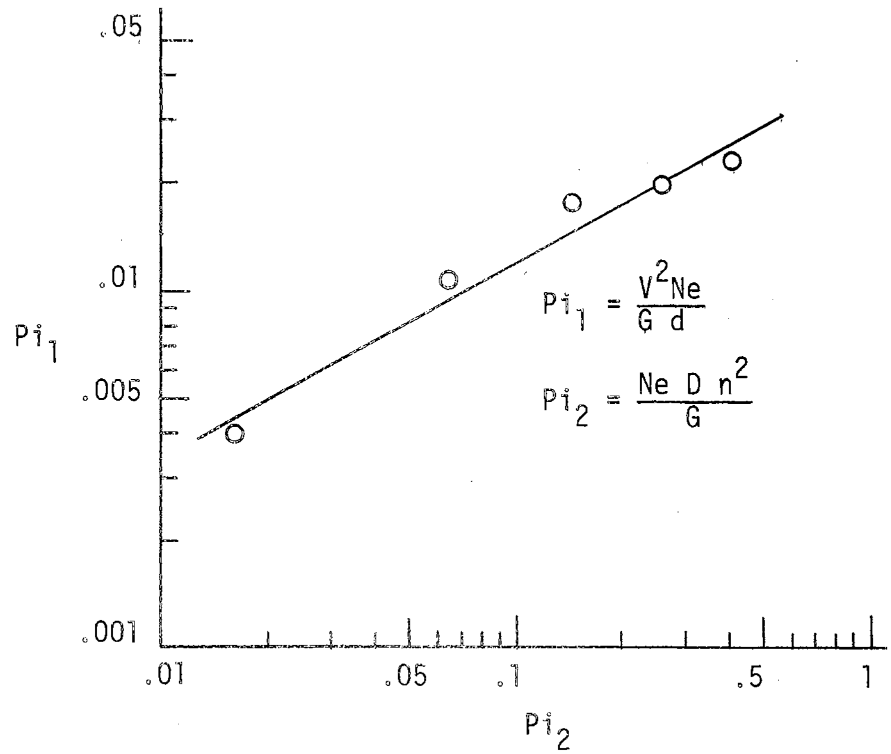

Figure 26. Plot of Pi_1 Versus Pi_2.

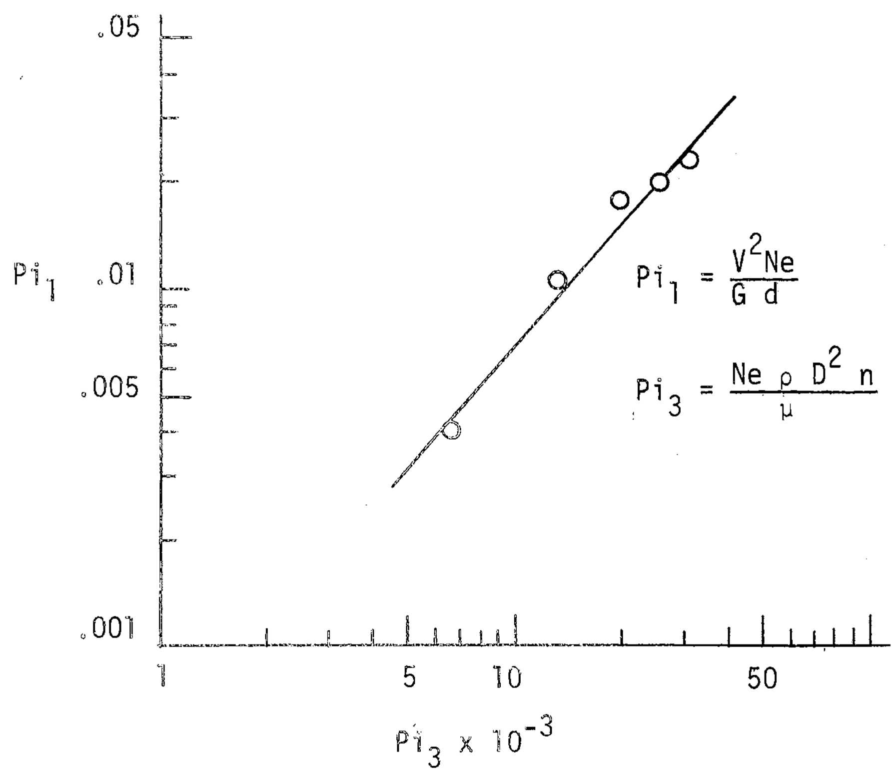

Figure 27. Plot of Pi_1 Versus Pi_3.

$$pi_1 = 0.0105\ (pi_4)^{-0.1904}$$

The correlation coefficient found for this equation was 0.998.

Pi_5 Analysis

As shown in Figure 29, plotting pi_1 against pi_5 $(\frac{P_{id}}{D})$ gave a straight line on log-log paper, with the equation of this relationship computed as:

$$pi_1 = 0.0549\ (pi_5)^{0.6579}$$

The correlation coefficient of this equation was calculated as 0.995.

Pi_6 Analysis

Plotting pi_1 against pi_6 $(\frac{D}{d})$ also gave a straight line plot on log-log paper, as shown in Figure 30. The equation computed for this relationship was:

$$pi_1 = 0.0254\ (pi_6)^{1.8355}$$

This equation gave a correlation coefficient between observed and computed pi_1 values of 0.994.

Pi_7 Analysis

As shown in Figure 31, a plot of pi_1 against pi_7 $(\frac{W_c}{L_c})$ failed to reveal a definite relationship between pi_1 and pi_7. Several equations expressing the relationship between pi_1 and pi_7 were developed, but all had correlation coefficients of less than 0.15. Thus, no equation relating pi_1 and pi_7 was included in development of the prediction equation for the model.

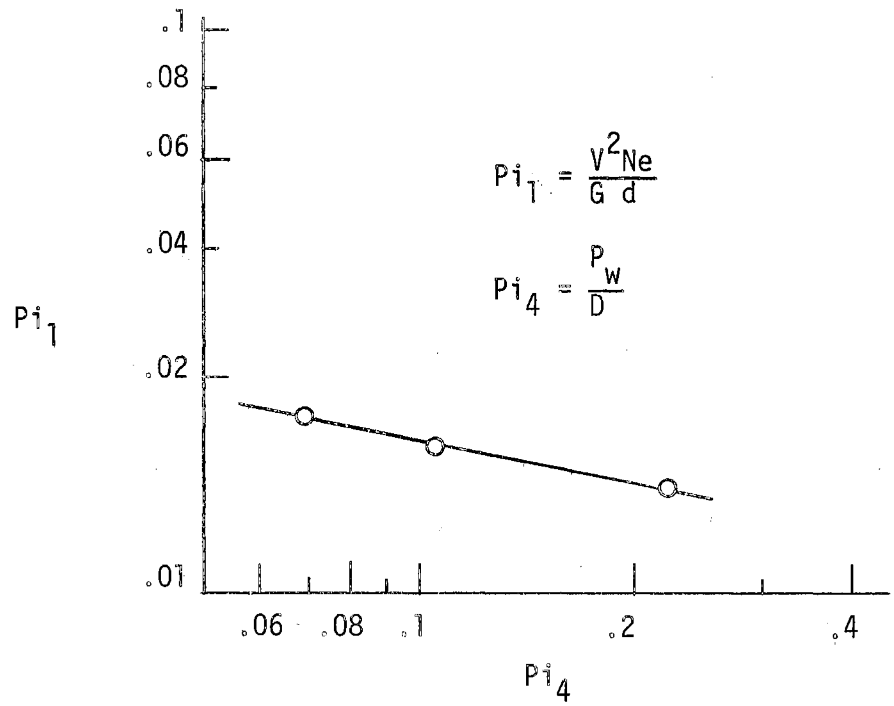

Figure 28. Plot of Pi_1 Versus Pi_4.

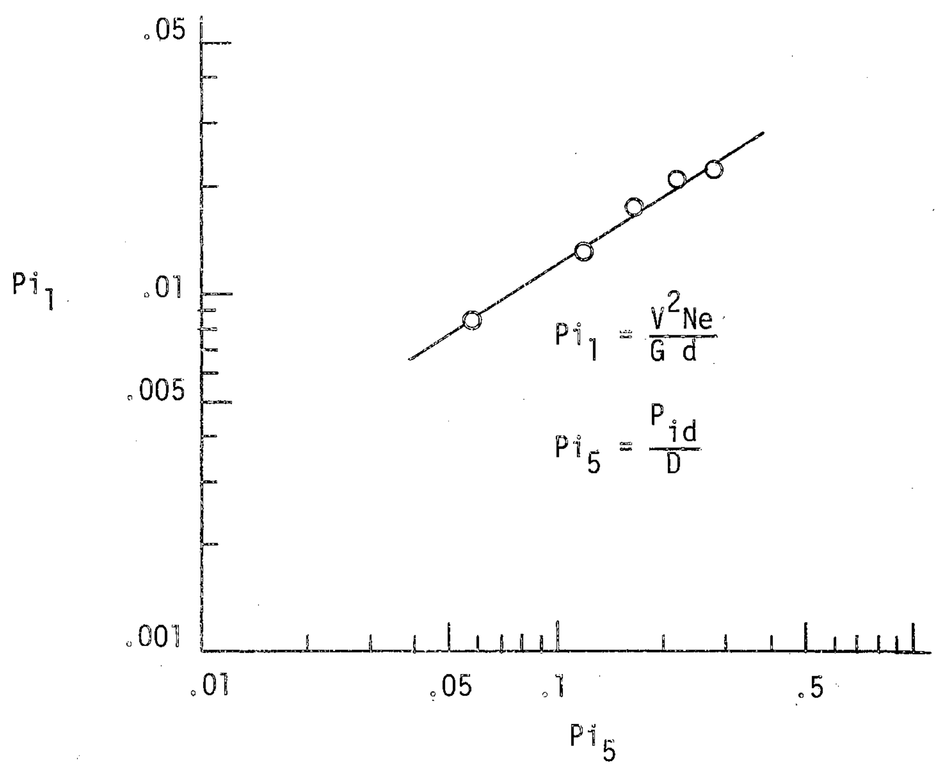

Figure 29. Plot of Pi_1 Versus Pi_5.

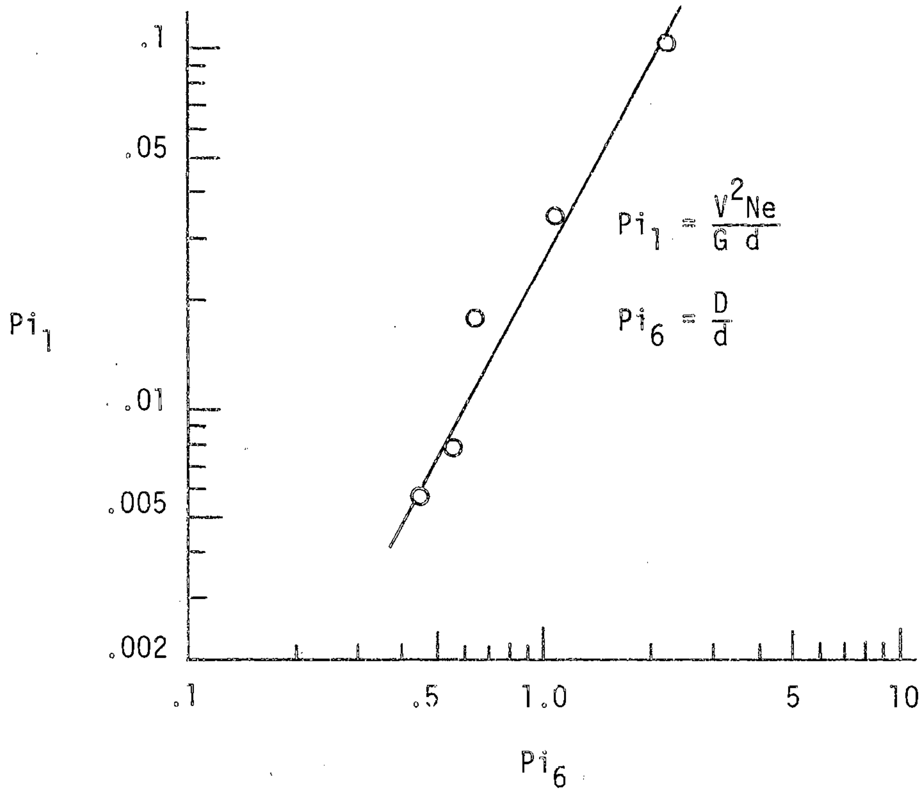

Figure 30. Plot of Pi_1 Versus Pi_6

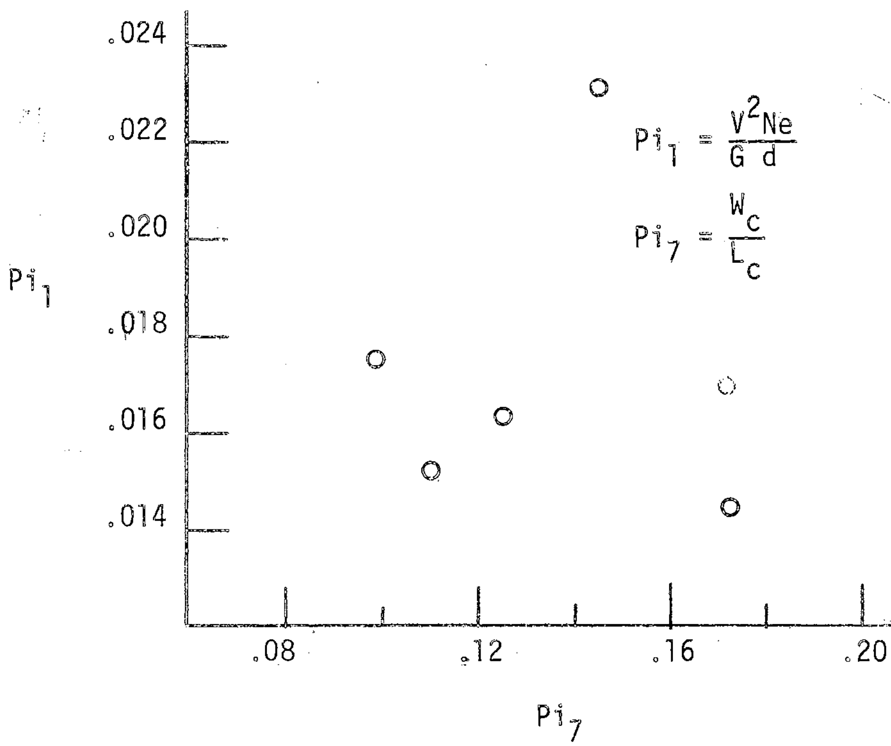

Figure 31. Plot of Pi_1 Versus Pi_7

Failure of the data to indicate a definite relationship between pi_1 and pi_7 may have been due to faulty technique in data collection. Since the uniformity of flow velocity across the channel width decreased as channel length decreased, the number of velocity traverses taken was probably insufficient and should have been increased.

Development of Prediction Equation

The prediction equation was developed by expressing the relationship between pi_1 and the independent pi terms in the following manner:

$$pi_1 = Q[f_2(pi_2) \times f_4(pi_4) \times f_5(pi_5) \times f_6(pi_6)]$$

where Q is a dimensionless constant, $f_2(pi_2)$ is the relationship found previously between pi_1 and pi_2, $f_4(pi_4)$ is the relationship between pi_1 and pi_4, etc.

This equation was changed to the form:

$$Q = \frac{pi_1}{f_2(pi_2) \times f_4(pi_4) \times f_5(pi_5) \times f_6(pi_6)}$$

and a value for Q found for each experimental run by substituting the proper values in for the pi terms for each test. The Q values obtained were averaged to determine a mean value of Q. This value and values for the component equations were then substituted into the equation, which was rewritten as given below:

$$pi_1 = 0.1498\,[(pi_2)^{0.5526} \times (pi_4)^{-0.1904} \times (pi_5)^{0.6579} \times (pi_6)^{1.8355}]$$

or,

$$\frac{V^2 Ne}{G\ d} = 0.1498\ [(\frac{Ne\ D\ n^2}{G})^{0.5526} \times (\frac{P_w}{D})^{-0.1904} \times$$

$$(\frac{P_{id}}{D})^{0.6579} \times (\frac{D}{d})^{1.8355}]$$

Using this equation, values of pi_1 were calculated for each experimental run and plotted against the observed pi_1 values on log-log paper, as shown in Figure 32. A linear regression analysis was conducted and a correlation coefficient between observed and calculated values of 0.979 was computed.

Discussion of Prediction Equation

Analysis of the prediction equation developed for the model indicates that, provided all other quantities are held constant at values normally associated with a prototype oxidation ditch, mean liquid velocity will:

1. Increase as rotor speed increases
2. Increase as paddle finger width decreases
3. Increase as immersion depth increases
4. Decrease as liquid depth increases

This behavior is illustrated by the graphs shown in Figures 33 and 34.

Comparison of mean velocity results found by Knight (13) in his investigation of the oxidation ditch at Iowa State University with the developed prediction equation does not clearly indicate whether the experimental model adequately represented this ditch.

The prediction equation indicates that increasing immersion depth increases mean liquid velocity in the ditch. Knight found that this relationship held for immersions of 6 inches or less, but found the mean velocity at 9-inch blade immersion to be slightly less than at

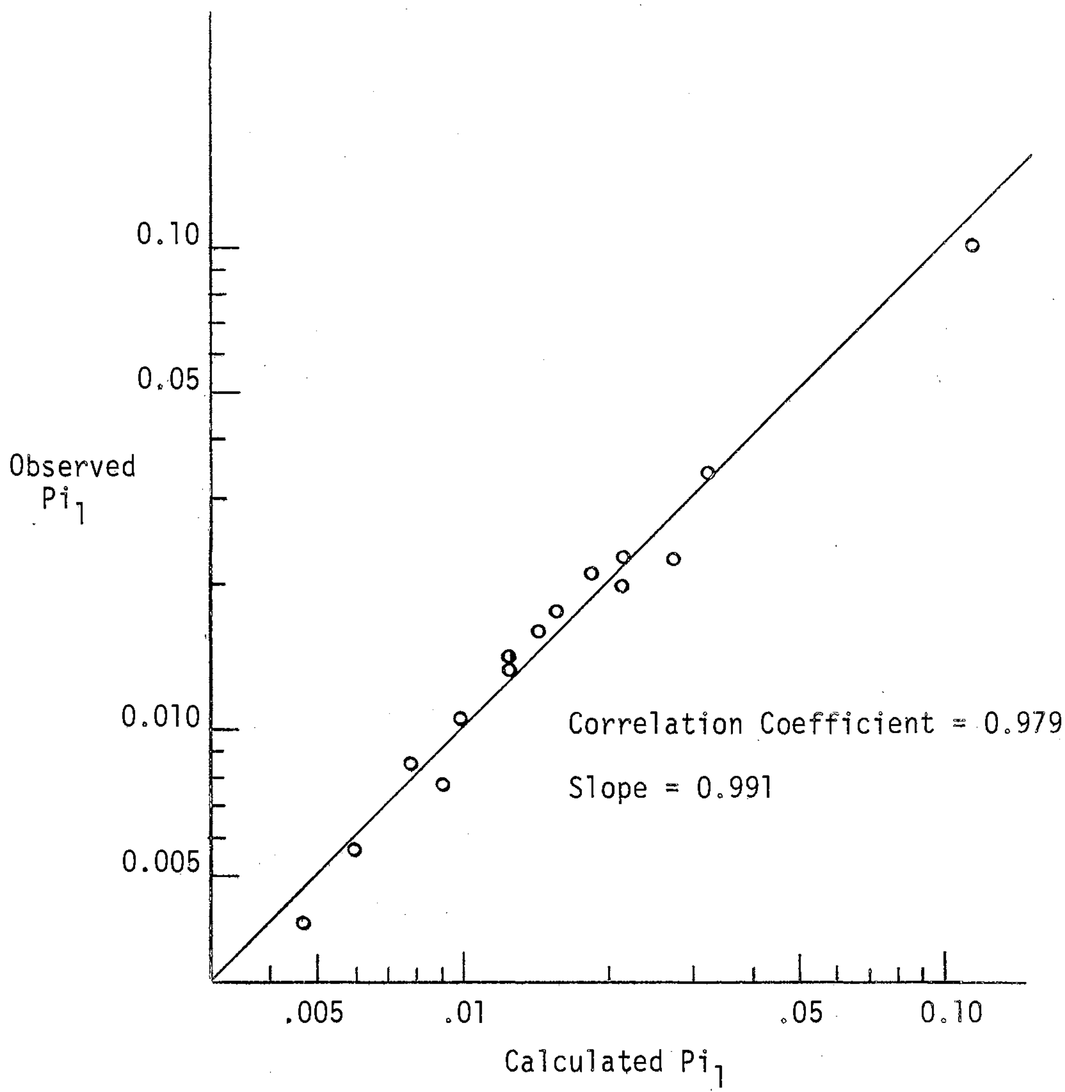

Figure 32. Plot of Observed Pi_1 Versus Calculated Pi_1.

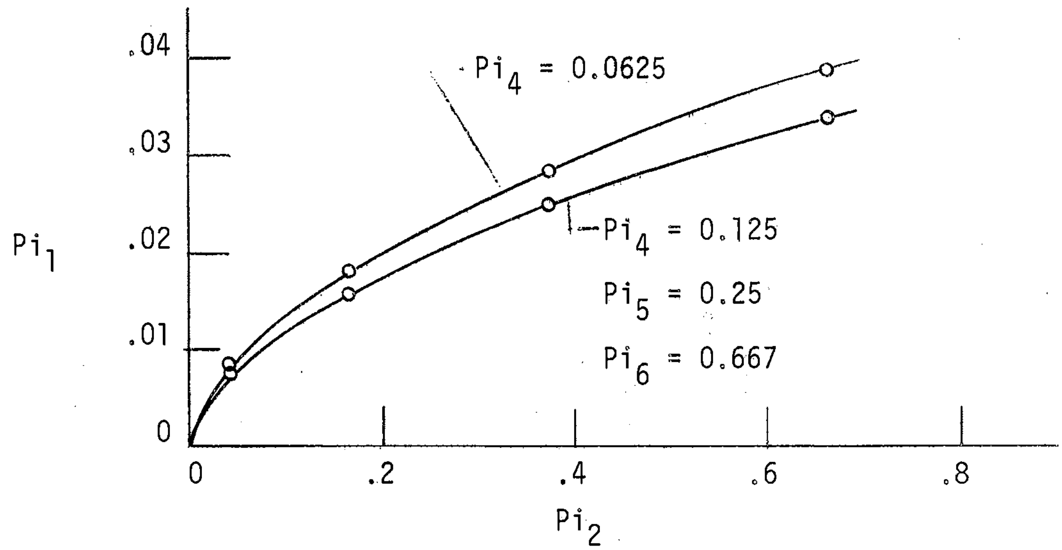

Figure 33. Graph Illustrating Behavior of Prediction Equation as Pi_2 and Pi_4 are Varied.

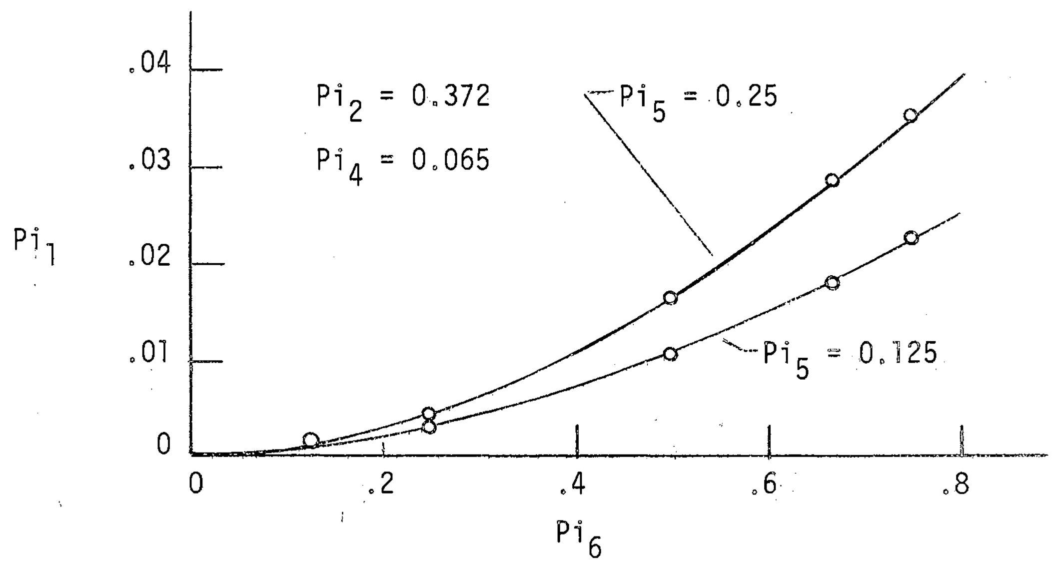

Figure 34. Graph Illustrating Behavior of Prediction Equation as Pi_5 and Pi_6 are Varied.

6-inch immersion and the mean velocity at 12-inch immersion depth to be less than at the 6- or 9-inch immersions but greater than at the 3-inch immersion. Whether this difference in behavior was due to failure of the model to adequately represent the prototype is unclear, as model tests were conducted at immersions representing prototype immersions of from 1.5 inches to 7.5 inches. Thus, this apparent inconsistency between the prediction equation and Knight's results may be due to prototype operation outside the range in which model tests were conducted.

An apparent difference between predicted and observed mean velocity results also exists when considering the effects of rotor speed on mean velocity. The prediction equation indicates that increasing rotor speed will increase mean velocity. Knight found this relationship to be true for immersions of less than 9 inches, but found a higher mean velocity at 60 rpm than at 100 rpm when operating at a 12-inch immersion depth. Again, this inconsistency may be due to operating at immersions outside the range for which the model tests were conducted.

Although insufficient prototype data existed to check the validity of the prediction equation, the available data was used to compare actual results in a prototype with results predicted by the equation.

Using data given by Knight (13), the mean liquid velocity and observed pi_1 value were computed for each prototype test conducted within the range of model tests. Also, by substituting prototype operating parameter values into the prediction equation, a calculated pi_1 value was obtained. (Prototype parameter values used and pi_1 values obtained are given in Table IX.) As shown in Figure 35, a plot of observed pi_1 versus calculated pi_1 indicates that calculated pi_1 values were generally slightly more than twice the observed pi_1 values.

TABLE IX

PROTOTYPE PARAMETER VALUES AND PI_1 VALUES

Rotor Speed (rpm)	Paddle Immersion (inches)	Mean Velocity (fps)	Pi_1 Observed	Pi_1 Calculated	Pi_1* Calculated
60	3	0.468	0.00136	0.00319	0.00152
60	6	0.665	0.00275	0.00505	0.00240
100	3	0.651	0.00264	0.00561	0.00266
100	6	0.808	0.00406	0.00887	0.00421

*Calculated Value of Pi_1 Using the Adjusted Prediction Equation

Rotor Diameter = 27.5 inches
Paddle Finger Width = 2.0 inches
Liquid Depth = 60 inches

A possible reason for this discrepancy between observed and calculated values is that geometric similarity did not exist between the model and prototype. Model tests were conducted in a rectangular channel, while the prototype channel had a trapezoidal shape. If the prediction equation were adjusted to compensate for this lack of similarity, the equation might better predict pi_1 values occurring in the prototype.

Several procedures could be used in attempting to compensate for this lack of similarity. One possible procedure would be to replace the liquid depth term in the equation with the channel hydraulic radius term. Another would be to change the value of the constant appearing in the equation.

This second procedure was used in attempting to fit the prediction equation to the prototype data. The average ratio of the observed pi_1 value to calculated pi_1 value was computed, and the constant in the prediction equation multiplied by this ratio. The adjusted prediction equation obtained by this procedure was:

$$\frac{V^2 Ne}{G\ d} = 0.0716\ [(\frac{Ne\ D\ n^2}{G})^{0.5526} \times (\frac{P_w}{D})^{-0.1904} \times$$

$$(\frac{P_{id}}{D})^{0.6579} \times (\frac{D}{d})^{1.8355}]$$

Using this adjusted equation, values of pi_1 were calculated and plotted against observed pi_1 values. As shown on the plot in Figure 36, the points fell near the 45° line, indicating that the adjusted equation could be used to predict the value of pi_1 for this prototype with a fair degree of accuracy. However, the available prototype data covered only

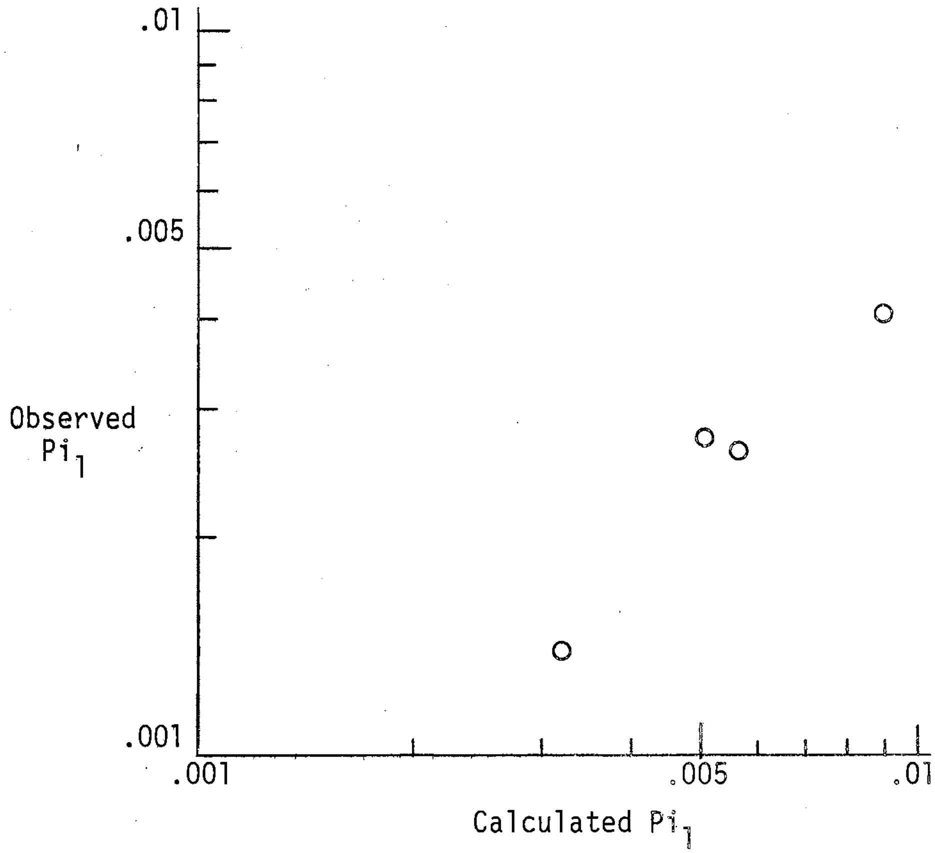

Figure 35. Observed Versus Calculated Prototype Pi_1 Values Using Developed Prediction Equation.

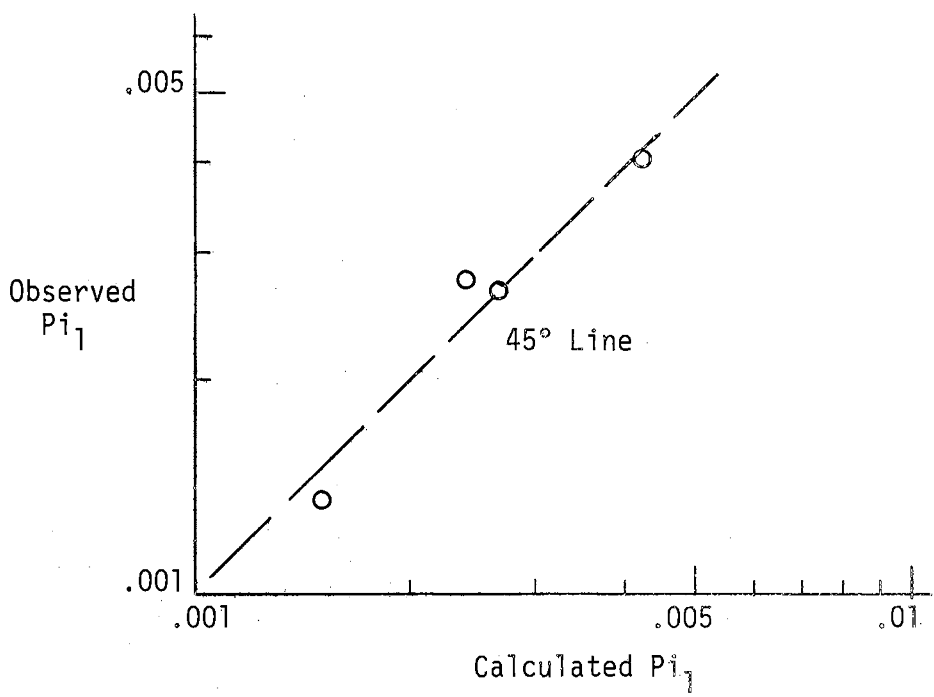

Figure 36. Observed Versus Calculated Prototype Pi_1 Values Using Adjusted Prediction Equation.

a small range of pi_1 values. The accuracy with which this equation could predict pi_1 values occurring in the prototype when operating outside of this pi_1 range is not known.

CHAPTER VIII

SUMMARY AND CONCLUSIONS

A model study of the velocities found in an oxidation ditch was conducted. The experimental investigation was organized and conducted according to similitude principles.

Equipment was developed and a procedure devised for measuring the velocity in the model at various horizontal and vertical positions across a section of the model. Velocity profiles were drawn and a mean velocity computed for the various tests.

The effects of changes in rotor speed, paddle finger width, paddle immersion depth, liquid depth, and channel length on the mean liquid velocity were investigated. It was found that, providing all other pertinent quantities were held constant, the mean liquid velocity:

1. Increased as rotor speed increased, with the rate of increase for a given speed change being greater at lower speeds than at higher speeds.
2. Increased as paddle finger width decreased, with the rate of increase for a given change in finger width being greater at smaller finger widths than at larger finger widths.
3. Increased as immersion depth increased, with the rate of increase for a given change in immersion depth being greater at low immersions than at high immersions.

4. Increased as liquid depth decreased, with the rate of increase for a given change in depth being greater at small depths than at large depths.

It was also observed that the uniformity of flow across a section of that channel not containing the rotor decreased as the channel length decreased.

A prediction equation was developed for the model. This equation was:

$$\frac{V^2\ Ne}{G\ d} = 0.1498\left[\left(\frac{Ne\ D\ n^2}{G}\right)^{0.5526} \times \left(\frac{P_w}{D}\right)^{-0.1904} \times \left(\frac{P_{id}}{D}\right)^{0.6579} \times \left(\frac{D}{d}\right)^{1.8355}\right]$$

An attempt to verify this equation thru use of data from a prototype ditch indicated that (provided adjustments are made in the equation to compensate for geometric differences between model and prototype) the equation could be used to predict the mean liquid velocity occurring in a prototype. However, insufficient data existed to conduct a complete verification of the equation.

Suggestions for Further Study

Since present recommendations are based primarily on experience with municipal sewage, the actual minimum velocity required to keep agricultural wastes in suspension should be determined.

The validity of the prediction equation developed in this study should be investigated by conducting tests on a prototype. A study should also be made relating the mean velocity obtained from an aeration rotor to the oxygenation capacity of the rotor.

A prototype study should be conducted to determine the effects various sedimentation pit designs will have on the operation of an oxidation ditch.

A further study should be conducted to determine the effect channel length has on the mean velocity in the oxidation ditch.

A study of the net rotor power requirements for various rotor and channel operating conditions should be conducted, with the study being conducted either in a prototype oxidation ditch or in a larger scale model than used in this investigation.

BIBLIOGRAPHY

1. Babbitt, H. E. and E. R. Baumann. Sewage and Sewage Treatment. 8th ed. New York: John Wiley and Sons, Inc., 1958.

2. Berk, W. L. Quality Treating with Economic First Cost. Lakeside Engineering Company Bulletin No. RAD-61. Chicago, Illinois.

3. Berk, W. L. Rotor Aeration, a Fresh Approach to an Old Problem. Lakeside Engineering Company Bulletin No. RAD-46. Chicago, Illinois.

4. Berry, E. C. "Requirements for Microbial Reduction of Farm Animal Wastes." Proceedings of National Symposium on Animal Waste Management. Publication No. SP-0366. St. Joseph, Michigan: American Society of Agricultural Engineers, 1966.

5. Curtis, D. R. "Design Criteria for Anaerobic Lagoons for Swine Manure Disposal." Proceedings of National Symposium on Animal Waste Management. Publication No. SP-0366. St. Joseph, Michigan: American Society of Agricultural Engineers, 1966.

6. Dale, A. C. and D. L. Day. "Some Aerobic Decomposition Properties of Dairy Cattle Manure." Paper No. 66-925. St. Joseph, Michigan: American Society of Agricultural Engineers, 1966.

7. Farm Effluents. Publication of National Agricultural Advisory Service. London: Ministry of Agriculture, Fisheries, and Food, 1964.

8. Hart, S. A. "Fowl Fecal Facts." World's Poultry Science Journal. 19: No. 4, October, 1963.

9. Hart, S. A. "Processing Agricultural Wastes." Paper presented at National Solid Waste Research Conference, Chicago, Illinois, December, 1963.

10. Hart, S. A. "Thin Spreading of Slurried Manures." Transactions of the American Society of Agricultural Engineers. 7: p. 22-28, 1964.

11. Hart, S. A., J. A. Moore, and W. F. Hale. "Pumping Manure Slurries." Proceedings of National Symposium on Animal Waste Management. Publication No. SP-0366. St. Joseph, Michigan: American Society of Agricultural Engineers, 1966.

12. Irgens, R. L. and D. L. Day. "Aerobic Treatment of Swine Waste." Proceedings of National Symposium on Animal Waste Management. Publication No. SP-0366. St. Joseph, Michigan: American Society of Agricultural Engineers, 1966.

13. Knight, R. S. "Performance of a Cage Rotor in an Oxidation Ditch." Unpublished M.S. thesis, Iowa State University, 1965.

14. Kolega, J. J., G. L. Nelson, and Q. B. Graves. "Rotor Aerator Design in Livestock Waste Management." Paper No. 66-929. St. Joseph, Michigan: American Society of Agricultural Engineers, 1966.

15. Lakeside Engineering Corporation. Rotor Aeration in the Oxidation Ditch. Bulletin 140. Chicago, Illinois.

16. Lawrence, N. A. "Mechanical Aeration is a Logical Development for Sewage Lagoons in Western Canada." Canadian Municipal Utilities. March, 1963.

17. Linn, A. "Whipping the Manure Problem." The Farm Quarterly. 21: No. 6, November, 1966.

18. Morris, W.H.M. "A Review of the Treatment of Manure in Oxidation Ditches." Research Progress Report, Agricultural Experiment Station, Purdue University, December, 1966. (Mimeo)

19. Morris, W.H.M. and T. W. Robinson. "The Economics of Disposal of Hog Manure in Confinement Systems." Paper No. 61-422, St. Joseph, Michigan: American Society of Agricultural Engineers, 1961.

20. Murphy, Glenn. Similitude in Engineering. New York: The Ronald Press Company, 1950.

21. Pasveer, A. Rotor Aeration, Lakeside Engineering Company Publication, Chicago, Illinois.

22. Rushton, J. H., E. W. Costhich, and H. J. Everett. "Power Characteristics of Mixing Impellors." Chemical Engineering Progress. 46: No. 8, p. 395-404, and 46: No. 9, p. 467-476, 1950.

23. Scheltinga, H.M.J. "Biological Treatment of Animal Wastes." Proceedings of National Symposium on Animal Waste Management. Publication No. SP-0366, St. Joseph, Michigan: American Society of Agricultural Engineers, 1966.

24. Sobel, A. T. "Physical Properties of Animal Manures Associated with Handling." Proceedings of National Symposium on Animal Waste Management. Publication No. SP-0366. St. Joseph, Michigan: American Society of Agricultural Engineers, 1966.

25. Steel, W. E. Water Supply and Sewerage. New York: McGraw-Hill Book Company, 1960.

26. Taiganides, E. P. and Thamon E. Hazen. "Physical and Chemical Properties of Animal Wastes." Paper No. 64-315. St. Joseph, Michigan: American Society of Agricultural Engineers, 1964.

27. Taiganides, E. P., et al. "Properties and Pumping Characteristics of Hog Wastes." Journal Paper No. J-4534 of the Iowa Agricultural and Home Economics Experiment Station. Ames, Iowa. March, 1963.

28. Webb, F. C. Biochemical Engineering. New York: D. Van Nortrand Company, Ltd., 1964.

29. Webster, N. W. and J. T. Clayton. "Operating Characteristics of Two Aerobic-Anaerobic Dairy Manure Treatment Systems." Proceedings of National Symposium on Animal Waste Management. Publication No. SP-0366. St. Joseph, Michigan: American Society of Agricultural Engineers, 1966.

30. Witzel, S. A., et al. "Physical, Chemical, and Bacteriological Properties of Farm Wastes." Proceedings of National Symposium on Animal Waste Management. Publication No. SP-0366. St. Joseph, Michigan: American Society of Agricultural Engineers, 1966.

APPENDIX A

VELOCITY MEASUREMENT DATA

APPENDIX A

VELOCITY MEASUREMENT DATA

Test No.	Measurement Depth-Distance Above Channel Bottom (inches)	Measured Velocity		
		Outside Traverse (fps)	Center-Line Traverse (fps)	Inside Traverse (fps)
1	0.167	0.146	0.146	0.127
	0.500	0.194	0.179	0.146
	0.833	0.194	0.194	0.146
	1.167	0.207	0.194	0.164
	1.500	0.207	0.207	0.146
	1.833	0.207	0.194	0.146
	2.167	0.220	0.194	0.127
	2.500	0.207	0.194	0.146
	2.833	0.207	0.207	0.146
2	0.167	0.264	0.243	0.220
	0.500	0.302	0.293	0.220
	0.833	0.322	0.322	0.243
	1.167	0.327	0.335	0.243
	1.500	0.327	0.335	0.243
	1.833	0.327	0.335	0.243
	2.167	0.335	0.335	0.231
	2.500	0.327	0.322	0.231
	2.833	0.327	0.322	0.231
3	0.167	0.322	0.327	0.274
	0.500	0.380	0.380	0.293
	0.833	0.414	0.414	0.311
	1.167	0.420	0.427	0.322
	1.500	0.433	0.433	0.327
	1.833	0.439	0.439	0.322
	2.167	0.433	0.420	0.311
	2.500	0.433	0.420	0.302
	2.833	0.433	0.414	0.293
4	0.167	0.373	0.366	0.284
	0.500	0.414	0.401	0.302
	0.833	0.451	0.433	0.322
	1.167	0.469	0.457	0.327
	1.500	0.474	0.463	0.327
	1.833	0.474	0.457	0.327
	2.167	0.480	0.445	0.311

Test No.	Measurement Depth-Distance Above Channel Bottom (inches)	Measured Velocity Outside Traverse (fps)	Center-Line Traverse (fps)	Inside Traverse (fps)
	2.500	0.469	0.439	0.302
	2.833	0.469	0.420	0.302
5	0.167	0.401	0.373	0.311
	0.500	0.445	0.420	0.335
	0.833	0.474	0.463	0.359
	1.167	0.491	0.480	0.366
	1.500	0.496	0.491	0.366
	1.833	0.496	0.480	0.366
	2.167	0.491	0.469	0.359
	2.500	0.486	0.463	0.351
	2.833	0.486	0.457	0.327
6	0.167	0.359	0.322	0.274
	0.500	0.380	0.359	0.284
	0.833	0.407	0.394	0.293
	1.167	0.420	0.420	0.302
	1.500	0.427	0.427	0.311
	1.833	0.433	0.427	0.302
	2.167	0.439	0.414	0.293
	2.500	0.433	0.407	0.284
	2.833	0.433	0.394	0.274
7	0.167	0.327	0.284	0.254
	0.500	0.366	0.322	0.254
	0.833	0.380	0.359	0.254
	1.167	0.387	0.373	0.274
	1.500	0.394	0.387	0.284
	1.833	0.401	0.387	0.274
	2.167	0.407	0.387	0.264
	2.500	0.401	0.380	0.264
	2.833	0.394	0.366	0.264
8	0.167	0.243	0.220	0.179
	0.500	0.274	0.274	0.207
	0.833	0.293	0.293	0.220
	1.167	0.302	0.302	0.220
	1.500	0.302	0.302	0.220
	1.833	0.302	0.293	0.220
	2.167	0.302	0.293	0.207
	2.500	0.293	0.284	0.207
	2.833	0.293	0.293	0.207
9	0.167	0.302	0.274	0.231
	0.500	0.335	0.322	0.254
	0.833	0.351	0.359	0.264
	1.167	0.373	0.366	0.284
	1.500	0.373	0.380	0.284
	1.833	0.380	0.373	0.284

Test No.	Measurement Depth-Distance Above Channel Bottom (inches)	Measured Velocity Outside Traverse (fps)	Measured Velocity Center-Line Traverse (fps)	Measured Velocity Inside Traverse (fps)
	2.167	0.380	0.366	0.274
	2.500	0.380	0.359	0.264
	2.833	0.373	0.359	0.254
10	0.167	0.380	0.359	0.302
	0.500	0.420	0.414	0.311
	0.833	0.451	0.439	0.335
	1.167	0.469	0.463	0.351
	1.500	0.469	0.469	0.351
	1.833	0.474	0.469	0.343
	2.167	0.474	0.463	0.335
	2.500	0.469	0.474	0.327
	2.833	0.463	0.469	0.327
11	0.167	0.414	0.359	0.293
	0.500	0.457	0.420	0.322
	0.833	0.491	0.457	0.351
	1.167	0.507	0.491	0.359
	1.500	0.507	0.502	0.359
	1.833	0.507	0.496	0.359
	2.167	0.507	0.486	0.335
	2.500	0.502	0.469	0.335
	2.833	0.502	0.463	0.327
12	0.167	0.538	0.486	0.420
	0.500	0.595	0.553	0.433
	0.833	0.634	0.599	0.445
13	0.167	0.407	0.394	0.343
	0.500	0.433	0.451	0.335
	0.833	0.469	0.486	0.351
	1.167	0.486	0.507	0.359
	1.500	0.491	0.523	0.366
	1.833	0.474	0.528	0.343
14	0.167	0.274	0.243	0.220
	0.500	0.302	0.284	0.220
	0.833	0.327	0.311	0.231
	1.167	0.327	0.327	0.243
	1.500	0.343	0.335	0.254
	1.833	0.343	0.327	0.243
	2.167	0.343	0.327	0.243
	2.500	0.343	0.322	0.243
	2.833	0.335	0.311	0.220
	3.167	0.335	0.302	0.207
	3.500	0.335	0.284	0.207
	3.833	0.327	0.284	0.194

Test No.	Measurement Depth-Distance Above Channel Bottom (inches)	Measured Velocity: Outside Traverse (fps)	Measured Velocity: Center-Line Traverse (fps)	Measured Velocity: Inside Traverse (fps)
15	0.167	0.264	0.231	0.220
	0.500	0.293	0.274	0.231
	0.833	0.322	0.293	0.231
	1.167	0.335	0.311	0.243
	1.500	0.327	0.322	0.243
	1.833	0.327	0.322	0.243
	2.167	0.327	0.311	0.231
	2.500	0.327	0.302	0.243
	2.833	0.327	0.293	0.243
	3.167	0.322	0.284	0.220
	3.500	0.322	0.284	0.220
	3.833	0.311	0.264	0.220
	4.167	0.311	0.264	0.207
	4.500	0.302	0.254	0.207
	4.833	0.302	0.264	0.207
16	0.167	0.335	0.327	0.264
	0.500	0.380	0.366	0.254
	0.833	0.394	0.394	0.274
	1.167	0.407	0.407	0.284
	1.500	0.414	0.414	0.284
	1.833	0.407	0.401	0.274
	2.167	0.401	0.394	0.274
	2.500	0.401	0.387	0.264
	2.833	0.401	0.380	0.254
17	0.167	0.366	0.366	0.264
	0.500	0.394	0.420	0.254
	0.833	0.414	0.433	0.243
	1.167	0.420	0.451	0.264
	1.500	0.414	0.445	0.264
	1.833	0.414	0.439	0.264
	2.167	0.414	0.427	0.264
	2.500	0.414	0.427	0.254
	2.833	0.407	0.420	0.254
18	0.167	0.420	0.407	0.414
	0.500	0.457	0.463	0.407
	0.833	0.451	0.474	0.407
	1.167	0.439	0.469	0.407
	1.500	0.420	0.457	0.407
	1.833	0.414	0.457	0.407
	2.167	0.414	0.457	0.414
	2.500	0.407	0.469	0.420
	2.833	0.407	0.480	0.420

Test No.	Measurement Depth-Distance Above Channel Bottom (inches)	Measured Velocity: Outside Traverse (fps)		Center-Line Traverse (fps)		Inside Traverse (fps)
19	0.167	0.491		0.457		0.104
	0.500	0.533		0.474		0.104
	0.833	0.512		0.451		0.074
	1.167	0.480		0.439		0.000
	1.500	0.469		0.433		0.000
	1.833	0.457		0.457		0.000
	2.167	0.420		0.502		0.104
	2.500	0.420		0.528		0.164
	2.833	0.414		0.558		0.164
20	0.167	0.401	0.672	0.502	0.264	0.127
(5	0.500	0.401	0.698	0.486	0.264	0.104
Traverses)	0.833	0.394	0.683	0.463	0.231	0.074
	1.167	0.373	0.675	0.457	0.194	0.074
	1.500	0.366	0.663	0.463	0.207	0.000
	1.833	0.359	0.650	0.496	0.231	0.000
	2.167	0.359	0.647	0.518	0.274	0.000
	2.500	0.351	0.625	0.553	0.311	0.000
	2.833	0.351	0.621	0.576	0.335	0.104

APPENDIX B

NET ROTOR POWER MEASUREMENT

APPENDIX B

NET ROTOR POWER MEASUREMENT

No measurements of net rotor power were obtained in this study, although several attempts to obtain this data were made. Attempts to obtain these measurements failed mainly because the net rotor power requirement was only a very small percentage of the total power input to the drive unit used for operating the rotor.

One method of power measurement investigated was based on the hypothesis that since the drive unit delivered a constant torque output, an increase in power requirements at the rotor should be accompanied by a decrease in the speed of motor (and subsequently rotor) rotation. It was planned to measure the rotor speed while operating in water and then lower the water level until the rotor was operating in air (which should increase the rotor rotation speed). A prony brake could then be used to apply load to the rotor shaft until rotor speed was again equal to that measured when operating in water. Then, by measuring the torque applied by the prony brake, a measure of torque on the rotor shaft due to operating in water would be obtained.

Attempts to utilize this method of measurement failed, as the difference in rotor speed between operating in water and in air was too small to be detected with the instruments available (a tachometer and a stroboscope were used).

Net rotor power could also be determined by measuring the voltage and amperage input to the motor when operating the rotor in air and in water. The difference in amperage input to the motor (at constant voltage) could be converted into net rotor power measurements by use of suitable equations. This method of measurement was also attempted, but failed. An ammeter with a scale range of 25 amps was used, and the amperage input to the motor was multiplied by a factor of 5 to use the total available scale range of the ammeter. Results indicated that the increase in amperage input to the motor due to operating in water as opposed to operating in air was less than 0.2 amps of a total amperage reading of between 20 and 21 amps. As this power difference was too small to measure accurately, this method was not used.

An effort was made to obtain a small DC motor capable of operating at the required rotor speeds. It was planned to drive the rotor by attaching it directly to the motor, thereby eliminating power losses occurring in the speed reduction unit and V-belt drive. Elimination of these losses would increase the percentage of total motor power input which was consumed as net rotor power requirement. However, no motor meeting the speed and torque requirements for the system was found.

Another method of measuring net rotor power considered was to measure the cumulative wattage input to the motor for a specified time period while operating the rotor in air and in water. The difference in wattage input would be a measure of net rotor power requirements. This method was not used, as the time period required for obtaining a significant wattage difference was felt excessive. Also, since voltage fluctuations occur in the electrical system of the shop facilities, this method would have required the measurement of these fluctuations and adjustment of cumulative input wattages to reflect these fluctuations.

VITA

Ubbo Agena

Candidate for the Degree of

Master of Science

Thesis: A MODEL STUDY OF FLOW VELOCITIES IN AN OXIDATION DITCH

Major Field: Agricultural Engineering

Biographical:

Personal Data: Born at Hampton, Iowa, August 29, 1944, the son of William H. and Eke H. Agena.

Education: Attended grade and high school at Dows, Iowa; graduated from Dows Community High School in 1962; received the Bachelor of Science degree in Agricultural Engineering in May, 1966, from Iowa State University; completed the requirements for the Master of Science degree in May, 1968.

Professional experience: During college--worked two summers as student trainee for Soil Conservation Service. After graduation--employed as drainage engineer with Wallace, Holland, Kastler, and Schmitz, Mason City, Iowa, for three months.

Professional organizations: Associate member of the American Society of Agricultural Engineers.